DEPARTAMENTO DE CIÊNCIAS DA VIDA

FACULDADE DE CIÊNCIAS E TECNOLOGIA
UNIVERSIDADE DE COIMBRA

Contribution of the ventro-lateral periaqueductal grey matter to fear conditioned analgesia

Dissertação apresentada à Universidade de Coimbra para cumprimento dos requesitos necessários à obtenção do grau de Mestre em Biologia Molecular e Celular, realizada sob a orientação científica do Doutor Cyril Herry (NeuroCentre Magendie, INSERM U862) e da Professora Doutora Ana Luisa Carvalho (Departamento de Ciências da Vida, Faculdade de Ciências e Tecnologia Universidade de Coimbra).

Nânci Aléxia Vieira Winke

2016

Funding Acknowledgments

O trabalho aqui apresentado foi realizado no Instituto NeuroCentre Magendie, INSERM U862, França, na equipa 'Neuronal circuits of associative learning' e financiado pela French National Research Agency (ANR-2010-BLAN-1442-01; ANR-10-EQPX-08 OPTOPATH; LABEX BRAIN ANR 10-LABX-43, LABEX TRAIL ANR 10-LABX-57), the European Research Council (ERC) under the European Union's Seventh Framework Program (FP7/2007-2013)/ERC grant agreement no. 281168, and the Conseil Regional d'Aquitaine ao Doutor Cyril Herry.

The work hereby presented was performed at the Institute NeuroCentre Magendie, INSERM U862, France, in the team of 'Neuronal circuits of associative learning' and funded by French National Research Agency (ANR-2010-BLAN-1442-01; ANR-10-EQPX-08 OPTOPATH; LABEX BRAIN ANR 10-LABX-43, LABEX TRAIL ANR 10-LABX-57), the European Research Council (ERC) under the European Union's Seventh Framework Program (FP7/2007-2013)/ERC grant agreement no. 281168, and the Conseil Regional d'Aquitaine.to Doctor Cyril Herry.

Acknowledgments

This study's development took place under the guidance of Cyril Herry and the supervision of Stephane Valerio. I am very thankful for both of their guidance, leadership, trust and help in pursuing this project in the laboratory under the best conditions.

I express my full and most sincere gratitude to Stephane, for the everlasting patience to answer all my 1001 questions per day. Without his direction I wouldn't have made it until here. He taught me that a negative result is as important as a positive result, and we had many of the former.

I would like to thank all my colleagues in Herry's team for all the support. To Einar Einarsson and Robert Rozeske, whom I shared the office with, thanks for the welcoming environment and the friendly encouragement and support along this year. I would also like to thank Hélène Wurtz and Fabrice Chaudun for their advice, assistance and kindness. A special thanks to Ana Santana for her friendship and for always having time to hear me, even when she actually did not have the time (obrigada irmãzinha!).

I also want to thank to the Portuguese research community in Bordeaux for all the dinners and beers and, more importantly, for the friendly atmosphere. A special thank you to my friends Alexandra and Filipe, who also embarked on this journey. I could have made it by myself but it would have been only half the fun.

I cannot forget all my master's degree colleagues. During this two years we panicked and then thrived together. We made it until the end! #aculpaédomestrado

I am very grateful for all the support and love from my friends, in particular Marina Ventura (who allowed me to have a cactus as a pet), Luís Gouveia and Francisco Pestana. Together we proved that friendship overcomes distance. A special thanks to Joana Ferreira, who is always present. There are not enough words to express how thankful I am for her friendship. My weeks without our talks would have been so boring: "I am an aspiring scientist during the day, a ninja at night and an astronaut on the weekends".

Last, but more importantly, I want to thank the two people without whom I would not be where I am today. To my parents, Emília Caetano e Fernando Almeida, I am very grateful for the infinite love and support. For always believing in me and giving me the freedom to make mistakes and learn with them. I could never forget my favourite artist, my little brother, Iago Almeida, whose energy never runs out. He is the person that I care the most in the world.

Table of Contents

List of Abbreviations

AAV	Adeno-associated virus
ACC	Anterior cingulate cortex
ANOVA	Analysis of variance
Aq	Aqueduct
Arch(T)	Archaerohodopsin
BLA	Basolateral amygdala
BR	Bacteriorhodopsin
ChR2	Channelrhodopsin2
CI	Conditioning index
Cre	Cyclization recombinase
CS	Conditioned stimulus
DAPI	4',6'-diamidino-2-phenylindole
DI	Discrimination index
DIO	Open-reading frame
dlPAG	Dorsolateral periaqueductal gray
dmPAG	Dorsomedial periaqueductal gray
EAA	Excitatory amino acids
EGFP	Enhanced green fluorescent protein
FCA	Fear conditioned analgesia
GABA	Gamma-aminobutyric acid
GAD	Glutamic acid decarboxylase
GFP	Green fluorescent protein
GPCRs	G-protein-coupled receptors
HP	Hot-plate
IITC	Incremental Hot/Cold Plate Analgesia Meter
IRES	Internal ribosome entry site
LED	Light-emitting diode
lPAG	Lateral periaqueductal gray
Mc	Magnocellular nucleus

MATLAB	Matrix laboratory
mPFC	Medial prefrontal cortex
NpRH	Halorhodopsin
OF	Open Field
PAG	Periaqueductal gray
PFA	Paraformaldehyde
PP	Place Preference
PTSD	Post-traumatic stress disorder
PVa^{+}	Parvalbumin positive cells
RSB+	Protonated retinal Schiff base
SC	Superior colliculus
SOM^{+}	Somatostatin positive cells
Thy1	Thy-1 membrane glycoprotein
TM	Transmembrane helix
US	Unconditioned stimulus
vlPAG	Ventrolateral periaqueductal gray

Abstract

Fear conditioned analgesia (FCA) can be defined as a reduction of pain sensitivity resulting from the exposure to a stimulus previously associated with an aversive event. Indeed, among the classically studied fear reactions - like freezing or avoidance – analgesia has been observed after fear conditioning although the underlying neuronal circuits are largely unknown. The ventro-lateral part of the periaqueductal grey (vlPAG) has been shown to be necessary for fear expression but is also considered as a key structure in descending modulation of pain. Thus, the vlPAG, which is highly connected to brain regions involved in fear processing (such as the amygdala and the medial prefrontal cortex) but also to the spinal cord, could be an interface between fear and pain behaviours observable in FCA. In this context, the present project had two main objectives: the first aim was to investigate further the behavioural paradigm of FCA recently established in the laboratory. We observed that animals submitted to a hot-plate (HP) test show a delayed response when the trial is paired with a conditioned stimulus (CS^+). This result suggests that CS^+-evoked fear responses can alter the animals pain threshold. We verified that this effect could not be due to a specific stress effect, and observed that FCA can be replicated with the same strength when the HP test is repeated. The second goal of the study was to test whether the vlPAG is involved in FCA. To do so, we used optogenetic tools to manipulate two populations of inhibitory interneurons: the somatostatin-expressing (SOM^+) and parvalbumin-expressing (PVa^+) interneurons. We observed that the activation of these two subpopulations induced a pro-nociceptive behavior, while the inhibition of PVa^+ interneurons induced an *analgesic-like* behaviour in the HP test. Importantly, these modulations of pain threshold were not any more visible when the animals were submitted to the FCA paradigm, suggesting that the fear-induced analgesia overcomes the optogenetic effects.

Key-words: **vlPAG; FCA; interneurons; neuronal circuitry.**

Resumo

Analgesia condicionada por medo (FCA) pode ser definida como uma redução da sensibilidade à dor resultante da exposição de um estímulo que foi previamente associado a um evento aversivo. De facto, entre as respostas clássicas de medo, como imobilidade ou fuga , analgesia tem também sido observada depois de medo condicionado. Contudo, os circuitos neuronais inerentes são ainda desconhecidos. Apesar da parte ventro-lateral da substancia cinzenta periaquedutal (vlPAG) ser necessária para a expressão de medo esta estrutura é também considerada essencial na modulação da via descendente da dor. Assim, a vlPAG é uma área que está extensivamente conectada a regiões neuronais envolvidas no processamento do medo (como por exemplo a amigdala e o cortex pre-frontal) mas também à medula espinal, podendo funcionar como uma interface entre as manifestações de medo e dor observados em FCA. Desse modo, o presente estudo teve dois objectivos principais: o primeiro foi estudar em detalhe o paradigma comportamental de FCA que foi recentemente estabelecido no laboratório. Nós observamos que os animais quando sujeitos ao teste de placa quente (HP) demonstram um atraso na resposta quando o teste é emparelhado com o estímulo condicionado (CS^+). Estes resultados sugerem que as respostas de medo elicitadas pelo CS^+ podem alterar os limiares de dor dos animais. Além disso, verificámos que estes resultados não foram causados devido a um efeito de stress especifico e que quando o HP teste é repetido a FCA pode ser replicada, mantendo a mesma intensidade de resposta. O segundo objectivo deste estudo foi testar se a vlPAG está envolvida em FCA. Para tal, usamos ferramentas de optogenética para manipular duas subpopulações de interneurónios inibitórios: interneurónios expressando somatostatina (SOM^+) e interneurónios expressando parvalbumina (PVa^+). No teste de HP, constatámos que a activação destas duas subpopulações induz um comportamento pró-nociceptivo, enquanto que a inibição dos interneurónios de PVa^+ resultam num comportamento analgésico. É importante salientar que a modulação destes limiares de dor não foi visível quando os animais foram submetidos ao paradigma de FCA, sugerindo que o efeito analgésico induzido por medo supera os efeitos da manipulação optogenética.

***Palavra-chaves*: vlPAG; FCA; interneurónios; circuitos neuronais.**

CHAPTER 1

INTRODUCTION

1. Introduction

Fear is a natural response to a threatening situation that leads to changes in behaviour, characterized as fear responses[1,2] and that enable the organism to avoid the threat and thus ensure its survival[1]. Typical fear responses include defensive behaviour[2], such as freezing or escape, but also autonomic responses (including changes in the arterial blood pressure and heart rate) and analgesia[3,4]. One of the most robust behavioural paradigm to study fear responses in the laboratory is Pavlovian auditory fear conditioning which consists in repeatedly associating a stimulus (such as a sound) with an aversive unconditioned stimulus (the US, such as a footshock). Following fear conditioning, the presentation of the stimulus alone (conditioned stimulus, CS) induces conditioned fear responses such a freezing or avoidance.

Interestingly, there is a strong overlap between the neuronal structures mediating fear conditioning and pain processing[5–8]. More specifically, the periaqueductal gray (PAG), the medial prefrontal cortex (mPFC) and the basolateral amygdala (BLA) are three central neuronal structures that have been involved both in fear behaviour and pain modulation[5–9]. Furthermore, several studies have shown that pain sensitivity can be modulated by fear, a phenomenon called fear conditioned analgesia (FCA)[5]. Several lines of evidence indicate that the PAG, specially the ventro-lateral part of the PAG (vlPAG) is a central structure in fear and pain modulation[10–12]. Indeed, the PAG is organized into four distinct longitudinal columns, referred as the dorsomedial (dmPAG), dorsolateral (dlPAG), lateral (lPAG) and ventrolateral (vlPAG) subdivisions, which are functionally different[10,13,14] (**Fig. 1**). In particular, the vlPAG is known to be involved in passive coping strategies, namely freezing, hyporeactivity and analgesia[10,13,15]. For instance, stimulation of the vlPAG through injections of excitatory amino acids (EAA) resulted in a decrease in pain sensitivity[4], via an opioid-dependent mechanism[12,15–17]. Moreover, lesions and pharmacological studies strongly suggested a role of the vlPAG in fear behaviour[18–20]. Specifically, electrical and chemical stimulation of the vlPAG produces defensive behaviour, particularly freezing. Thus, the vlPAG is an ideal structure in which the neuronal circuits underlying fear and pain may strongly overlap.

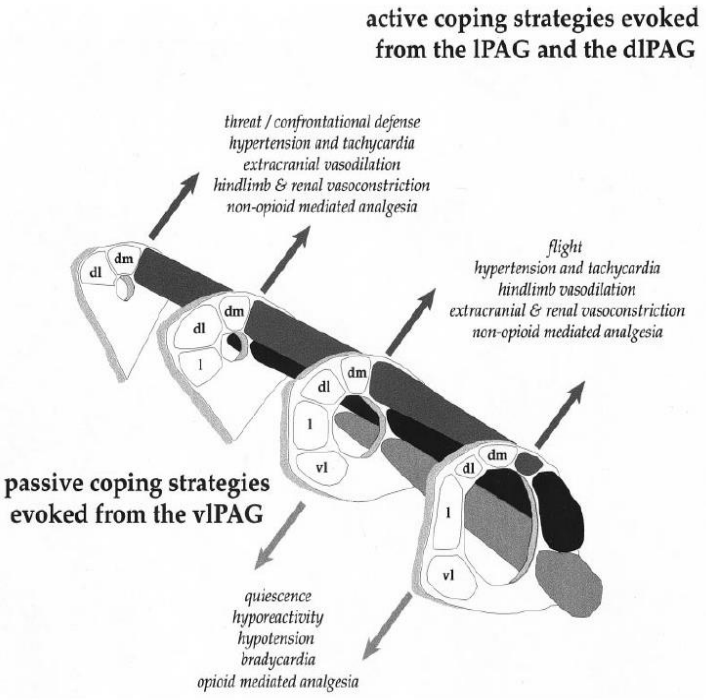

Figure 1. Schematic representation of the dorsomedial (dmPAG), dorsolateral (dlPAG), lateral (lPAG) and ventrolateral (vlPAG) neuronal columns within the PAG. Active and passive strategies evoked, respectively, from the dl/lPAG (lPAG – black colour) and the vlPAG (grey colour). Adapted from Bandler et. al, 2000[10].

Importanlty, a recent study identified for the first time the precise microcircuits in the vlPAG recruited during freezing behaviour[21]. In this report, the authors characterized a pathway from the central lateral amygdala to the PAG that produces freezing through disinhibition of the vlPAG excitatory outputs to the magnocellular nucleus (Mc) of the medulla. Moreover, they also show that the specific activation of excitatory $VGlut^{2+}$ neurons in vlPAG induced analgesia. Therefore these findings are, to our knowledge, the first clear demonstration of the existence of a local mircrocircuit in the vlPAG that can produce both freezing and analgesia, two important elements of the defensive response to threat.

FCA can be operationally defined as a decreased of pain sensibility upon re-exposure to a stimulus previously paired with a nociceptive US[5]. Early studies validated this phenomenon in which analgesia could be induced by a stressful stimulus[4,3]. Additional investigations revealed that analgesia could be induced both by natural threats (exposure to a predator) and conditioned fear. For instance, re-exposition to the conditioning context following conditioning lead to analgesia as measured in the tail-flick test or in the formalin injection test[4]. However, these studies did not manipulate the precise neuronal circuits involved in the vlPAG during FCA.

From a clinical standpoint, recent studies in humans revealed that individuals suffering from post-traumatic stress disorder (PTSD), the most common anxiety disorder, displayed a change in pain sensitivity when compared to individuals with other anxiety disorders[23] or healthy controls[23,24]. These results suggest a strong interplay between the neuronal circuits mediating fear and pain behaviour, which alteration could promote the development of this pathology. However, to date, the precise neuronal circuits and mechanisms controlling the interaction between fear and pain behaviour are still largely unknown. To address this question we used a combination of behavioural and optogenetic approaches to investigate the interactions between fear and pain networks in the vlPAG. ***The objectives of this project were twofold. First, to develop and validate the FCA behavioural paradigm in our laboratory and second to examine the contribution of vlPAG in both pain sensitivity and FCA .***To achieve our objectives, mice were submitted to a FCA protocol during which they first experienced classical Pavlovian fear conditioning and were submitted later to a Hot Plate (HP) paradigm. During auditory fear conditioning, the CS acquires aversive properties.The capacity of the CS to induced analgesia was subsequently assessed in the HP test by measuring the latency to observe a pain response (delayed response in case of analgesia). To causally test the involvement of the vlPAG in FCA we used optogenetic approaches to activate or inactivate the vlPAG by selectively activating two main populations of inhibitory interneurons: somatostatin-expressing (SOM^+) and parvalbumin-expressing interneurons (PVa^+).

CHAPTER 2

MATERIAL and METHODS

2. Material and Methods

Animals

Male C57BL6/J, SOM-IRES-Cre mice and PVa-IRES-Cre mice were individually housed, under a 12 h light/dark cycle, and provided with water and food *ad libitum*. Before experiments, animals were handled daily for at least five days. All procedures were performed in accordance with standard ethical guidelines (European Communities Directive 86/60-EEC) and were approved by the committee on Animal Health and Care of Institut National de la Santé et de la Recherche Médicale and French Ministry of Agriculture and Forestry (authorization A3312001).

Fear Conditioning

Apparatus – Fear Conditioning took place in two different contexts (context A and B). The habituation and fear retrieval sessions were conducted in Context B whereas the conditioning session occurred in context A. The context boxes A and B were cleaned, respectively, with 70% ethanol or 1% acetic acid before and after each session. The shapes of the two experimental boxes were also different with context A being a transparent Plexiglas square shape (diameter: 25 cm, height: 40 cm) with an electrical grid floor, while context B consisted in a transparent Plexiglas cylindrical shape (diameter: 25 cm, height: 24 cm) with a plastic floor. Additionally, light was reduced in context B to maximize contextual discrimination. Both context boxes were closed in a sound-attenuated cubicle. To score freezing behaviour, we used an automated infrared beam detection system located on the bottom of the experimental boxes, placed 1 cm above the flooring. The mice were considered to be freezing if no movement, except respiratory movement, was detected for at least 1 s.

Protocol – On the first day, mice were submitted to a habituation session, where two different CSs were played four times each. Each CS lasts 30 s and was composed of 27 pips (50 ms), presented at a frequency of 0.9 Hz. The pip frequency was either white-noise (CS^-) or 7.5 kHz (CS^+) with an intensity of 80 dB sound pressure level. During the fear conditioning session the animals were submitted to five CS^+–US pairings (inter-trial interval > 20 sec and < 180 sec: US: 1 sec.; 0,45 mA). The onset of the US coincided with the offset of the CS^+. The CS^- was presented after each CS^+–US pairing, but never reinforced, giving a total of five CS^-

presentations. Twenty-four hours later, the animals were submitted to a fear retrieval session, during which they received four presentations of the CS^- and CS^+ alone (**Fig. 2**). Freezing behaviour was measured during each session. Because we were interested in the modulation of pain sensitivity by fear, it was mandatory to evaluate associative fear levels following conditioning before assessing its impact on pain sensitivity. To evaluate conditioning, we computed two indices, the discrimination index (DI), which allow to identify if following conditioning mice discriminated between the CS^- and CS^+, and the conditioning index (CI), which provide an indication of whether the mice froze to the CS^+. These indexes were calculated as follows: $DI = \frac{(Freezing\ to\ CS+)-(Freezing\ to\ CS-)}{(Freezing\ to\ CS+)+(Freezing\ to\ CS-)}$ and CI = DI × (Freezing to CS^+).

Based on previous experiments realized in the laboratory, animals were considered conditioned if either their DI > 0.4 or CI > 0.15. The animals that did not reach these values were reconditioned before undergoing the HP test.

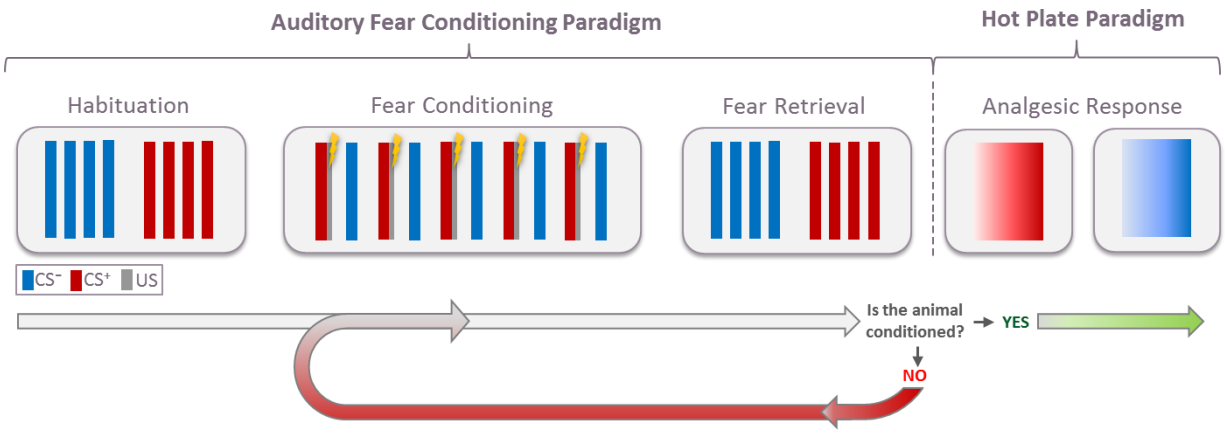

Figure 2 – Behaviour protocol. The protocol is a combination of two steps: 1) Auditory fear conditioning; 2) Hot Plate test. The Auditory fear conditioning consists in three sessions: an Habituation session in which the two tones are presented in a sequential manner ($4CS^-/4CS^+$)., a Conditioning session performed in a different context and during which the CS^+ is paired with a mild footstock (US onset started at the end of the $CS^{+)}$ and a Retrieval session which consisted in the presentation of 4 CS^- followed by the presentation of the 4 CS^+. If the animal is conditioned (evaluated by discrimination and the conditioning indices) it was submitted to the Hot Plate Paradigm, if not, the animal was re-conditioned. The hot-plate paradigm consisted in two trials, in which one of the two tones (counterbalanced between animals) is presented while the temperature increases (6ºC/min).

Hot Plate Test

Apparatus **–** We used an incremental Hot/Cold Plate Analgesia Meter (IITC) with a testing surface of 10 cm width per 20.3 cm length. The testing surface was located within a quadrangular Plexiglas box (height: 20.5 cm) in order to restrain the animal during the HP session. A speaker was attached to this structure to deliver the tones, (white-noise or 7.5 kHz). A white house light

and a video camera, which was connected to a computer, were positioned in a way that both the animal and the front panel of the HP device could be observed during the entire procedure. The temperature of the mice and its surroundings were recorded with an infrared digital thermographic camera (Testo 885) that was placed ~50 cm above the HP. The thermal camera has a spatial resolution of 320 × 240 pixels, a sampling rate of 25 Hz and a thermal sensitivity of 0.03° at 30°C. The thermographic recordings were analysed offline using the Testo IRSof software. The entire equipment was placed in a sound-attenuated box. The mice were considered to display a nociceptive response when jumping or licking their hind paws and this behaviour terminated the HP session.

Protocol – For FCA the mice were submitted to the HP session following fear conditioning **(Fig. 2)**. Each animal underwent two HP trials, one when the CS^+ was played (HP_CS^+) and one while the CS^- was played (HP_CS^-). The two trials were counterbalanced among animals. The animals were placed in the HP for 60 sec while the plate had a temperature of 30°C. Then the HP temperature gradually increased (rate: 6^o C per minute) until the animal displays the nociceptive response (jump or licking on of their hind paws). The tone (CS^+ or CS^-) was displayed 130 s after the HP was started and lasted until a nociceptive response was observed. A cut-off temperature of 60 ^{o}C was set to avoid permanent lesions to the mice tail and paws. The effect of fear on pain sensitivity was assessed by comparing the nociceptive temperature observed in the two HP trials: $[\Delta HP= (HP\_CS^+)-(HP\_CS^-)]$.

In the optogenetic experiments for FCA, each animal underwent two HP trials, during which one of the tones was played at the same time that light stimulation was delivered. Half of the animals received the light stimulation while the other half did not receive the light stimulation but had the fibers connected. The CSs was counterbalanced. In order to assess the effect of vlPAG optogenetic manipulation on pain sensitivity, the HP was also performed without auditory stimulus. In this case the optical stimulation was delivered 130 s after the HP was started and continued until a nociceptive response was observed.

Open field

***Apparatus* –** The Open Field (OF) was a control aimed to test the locomotion for the *light-stimulation* effect. The OF had a testing surface of 38 cm width per 38 cm length and was enclosed in a quadrangular Plexiglas box (height: 25 cm) in order to restrain the animal during the OF session. The floor of the arena was movable so that it could be cleaned in between animals. A red LED was attached to one of the side of the Plexiglas walls in order to signal the beginning and ending point of each session. The same LED was also used to signal the optical light stimulation. A white house light and a video camera, which was connected to a computer, were positioned above the arena so that the animal could be recorded for subsequent offline analyses. The entire equipment was placed in a sound-attenuated box. For each animal the distance travelled and the time spent in either the center or periphery of the arena was computed with a free user videotracking software (idTracker: Tracking individuals in a group by automatic identification of unmarked animals) and further analysed with MATLAB.

***Protocol* –** The OF test consisted of a 9-min trial divided in 3-min epochs. During epoch 1 and epoch 3 no light was delivered: the animal activity during these two epochs will be compared to the one observed in epoch 2 when light stimulation is displayed. Each animal underwent one OF session with two trials to counterbalance the *light* effect: one trial with optical stimulation and another without optical stimulation. The two trials were necessary to control for the animal locomotion during the total time of the epochs. If the mice change their locomotion activity between *epochs* but not between *light* trials one should observe the effect on the *control* trial (without optical stimulation). The two trials were executed on the same day with a minimum 3 h interval between the trials. The two types of trials were counterbalanced among animals. The first and third epoch for the *light* trial were considered, respectively, as pre-stimulation (*Pre-Stim*) and post-stimulation (*Post-Stim*), while the second was the epoch of optical stimulation (*Stim*). The total distances travelled by the animal during each epoch were calculated. For further analysis, the OF chamber was divided into a centre field (center) and an outer field (periphery), both equal in area.

Place Preference

***Apparatus* –** The Place Preference apparatus (PP) was a control intended to test the aversipm for the *light-stimulation* effect. The PP consisted in two inter-connected chambers, each with an area of 470 cm^2 and 25 cm of height. Each chamber was made out of Plexiglas and the walls were labelled with black/white stripes (Box 1) or no stripes (Box 2). The movable wall that connected the chambers was completely black on the side of Box 1 and white on Box 2. The floor of the arena was the same for both boxes. A white house light and a video camera, which was connected to a computer, were positioned above the arena so that it could be recorded for subsequent analyses. The entire equipment was placed in a sound-attenuated box.

***Protocol* –** The PP consisted in two sessions composed of three trials. Day 1 began with a *baseline* trial, followed by the light *stimulation* trial, separated by at least 3 h. On day 2 the third trial was the *test* trial (Post stimulation). During the *baseline* trial, the mice were placed in the chambers to freely explore the entire apparatus for 6 min. No light stimulation was delivered in the *baseline* trial. During the *stimulation* trial, the mice were confined to one of the two chambers for 3 min and received light stimulation. Stimulation in the Box 1 and Box 2 was counterbalanced across mice. During the *test* trial, the mice were again placed in the chambers to freely explore the entire apparatus for 6 min. Each animal was submitted to two sessions, one with light stimulation and another without light stimulation. The order of the sessions was counterbalanced across mice. The time spent by the mice in the two chambers were measured and used to quantify PP.

Optogenetics

***Viral injections* –** For optogenetic manipulation, SOM-IRES-Cre mice received stereotaxic injections of AAV viruses encoding for channelrhodopsin2 (ChR2, AAV-EF1a-DIO-hChR2(H134R)-EYFP, serotype 5, Vector Core, University of North Carolina) in the vlPAG whereas PVa-IRES-Cre mice received stereotaxic injections of AAV viruses encoding for either ChR2 (AAV-EF1a-DIO-hChR2(H134R)-EYFP, serotype 5, Vector Core, University of North Carolina) or ArchT (AAV-FLEX-ArchT-GFP, serotype 9,Vector Core, University of North Carolina) in the vlPAG. Control SOM-IRES-Cre and PVa-IRES-Cre received stereotaxic

injections of a control AAV encoding for GFP (AAV-FLEX-GFP, serotype 5; Vector Core, University of North Carolina).

Animals were anesthetized with isoflurane (induction 3%, maintenance of 1.5%) during the entire surgery to assure complete inhibition of reflexes. Animals were held in a stereotaxic frame (Kopf) and the body temperature was maintained between 32 – 37°C and monitored with a DC temperature controller system (FHC). Before the surgical incision, the area was clean with betadine and an ophthalmic gel (Lacrigel) was applied to the eyes in order to prevent drying during the surgery. A local injection of 0.05 ml of the local anaesthetic Lurocaine was given in the subcutaneous space above the skull before incision. The viral injection was performed at the following coordinates from Bregma (Franklin and Paxinos, 2012[25]): - 4.70 anterior-posterior, ± 0.65 medial-lateral and - 2.2 dorso-ventral. A single-barrel pipette of standard glass capillary with a tip diameter of 30 µm was filled with the AAV virus and lowered to the injection site through a motorized micromanipulator (LinLab software, Scientifica). The pipette was held in the right coordinates 2 minutes before the injection. Afterwards, 0.3 µl of virus was injected in each side of the brain and the pipette was held for 5 minutes between the injections to allow for a proper diffusion of the AAV virus. The skin was stitched and an antibacterial cream (Sulmidol, active substance: sulfapyridine) was applied to prevent infection. The animals were allowed to recover from the anaesthesia in a warm ventilated box.

Optic fiber implantation **–** Between 14 and 16 days after viral injections, mice were anesthetized and the skull was exposed using the same protocol as described above. Three stainless steel screws were fixed to the skull in order to support the head implant. Two optic fibers (0.48 numerical aperture, 200 µm diameter, Thorlabs) were implanted above the vlPAG at the following coordinates from Bregma (Franklin and Paxinos, 2012[25]): - 4.70 anterior-posterior, ± 0.65 medial-lateral and – 1.7 dorso-ventral. The optic fiber was lowered into the brain with an angle of 8^0. Next, the optic fibers were fixed to the skull with white-opaque dental cement (Super-Bond C&B). A layer of black-opaque varnish was applied over the dental cement to prevent passage of light. The incision was sutured and the same antibacterial cream as described above was applied to the areas surrounding the suture. After surgery, mice were allowed to recover one week to ensure sufficient expression of the opsins. Then, the animals were handled during one additional week. Mice started the behavioural training four weeks after viral injection.

Optical stimulation **–** A laser (IkeCool Corporation) was used to generate a blue light at 473 nm or a yellow light at 593 nm and connected to a 200 µm diameter optic fiber and calibrated to produce a tip irradiance of 10 to 12 mW. The timing, the frequency and the pulse duration were controlled via a software (Imetronic). After auditory fear conditioning, the animals were submitted to a HP test in which the tones (CS^+ and CS^-) were paired with light stimulation. To ensure that animals could move freely, the connecting fibers were suspended over the behavioural apparatus and attached to a commutator. Several parameters were tested for both SOM-IRES-Cre mice and PVa-IRES-Cre mice during the duration of the experiments. Table 1 summarizes the stimulation parameters used in the different behavioural sessions:

Table 1 – Summary of the different stimulation parameters used with the SOM-IRES-Cre mice and the PVa-IRES-Cre mice in the different behaviours tests of this study.

	SOM-IRES-Cre mice			PVa-IRES-Cre mice	
	5 ms pulse 5 Hz (ChR2)	50 ms pulse 5 Hz (ChR2)	5 ms pulse 2 Hz (ChR2)	40 ms pulse 20 Hz (ChR2)	Continuous (ArchT)
HP	√	√	√	√	√
FCA	√	-	-	√	√

Perfusion and Histology

Animals were enclosed in a box containing a lethal amount of isoflurane and subsequently perfused with 4% paraformaldehyde (PFA) diluted in 0.1 M phosphate buffered saline, pH = 7.2. The perfusion was executed with a peristaltic pump at a rate of 2 mL/min. Once the perfusion was completed the animal was decapitated. The brain was carefully removed. Afterwards the brain was placed in 4% PFA during 24h at 4º C. The brain was then placed in PBS until it was cut. Slices of 80 µm were cut using a vibratome (Leica), mounted on slides and coverslipped with a medium for fluorescence with 4',6'-diamidino-2-phenylindole (DAPI) (Vectashield, Vector Laborotories, Inc.). An upright microscope (Model BX43F, Olympus, Life Science) was used to identify the location of the optic fibers and the site of viral injection in the brain. In the animals

where the site of virus injection and/or fibers location was outside the vlPAG, those animals were removed from analysis.

Analysis

The mean percentage of freezing during the fear retrieval test and the temperatures in the HP during CS presentations were compared using a Repeated-Measures ANOVA ($P < 0.05$). Student t-tests were used to analyse the CI and the HP, both with and without CSs. The post-hoc test Student-Newman-Keuls was used for further analyses. Because no significant difference was found between them, animals that were infected with either ChR2 or ArchT but not stimulated, were pooled with the animals infected with GFP (that either underwent the behaviour with or without optical stimulation) as *Control.*

CHAPTER 3

EXPERIMENTS and RESULTS

3. Experiments and Results

Preliminary results: the *analgesic-like* effect of a fear conditioned stimulus

FCA is a phenomenon that has already been demonstrated in mice[5] although there is only few publications available. Therefore, it is important to test whether in our experimental conditions, the fear conditioning procedure induces analgesia in the HP test.

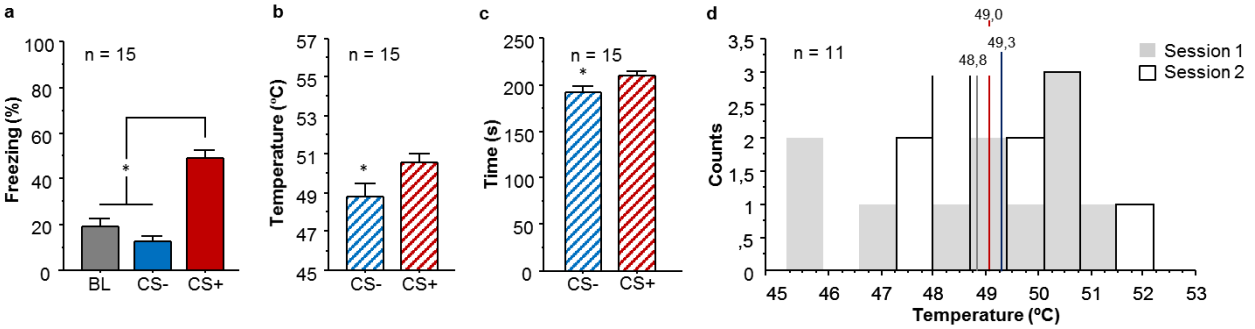

Figure 3 – Fear Conditioned Analgesia. a. Mean percentage of freezing observed for conditioned animals during the fear retrieval session. In the fear retrieval session, mice (n = 15) exhibited high freezing levels for the CS^+ but not for the baseline nor the CS^- (Repeated Measures ANOVA, $F_{(2,28)}$ = 77.368, P < 0.0001). Post-hoc Student-Newman-Keuls revealed significant differences between CS^+ and all other conditions. **b.** Mean temperatures for mice (n = 15) at which a *nociception-like* response was observed in the HP test. Nociceptive response was seen at a significantly higher temperature for the CS^+ trial compared to the CS^- trials (Repeated Measures ANOVA, $F_{(1,14)}$ = 7.037, P < 0.0189). **c.** Mean latency at which a *nociception-like* response was observed in the HP test. Nociceptive response occurred significant earlier for the CS^- trial than for the CS^+ (Repeated Measures ANOVA, $F_{(1,14)}$ = 7.396, P < 0.0166). **d.** Distribution of the temperature during the CS^-. Each animal (n = 11) were subjected to two trials in which the CS^- tone was played, there were no significant differences between the two trials (Repeated Measured ANOVA, $F_{(1,10)}$ = 0.640, P = 0.4424). The mean temperature for the trial 1 and 2 were 48.8°C and 49.3°C, respectively. The total mean temperature during the entire session was 49.0 °C (red vertical line). Error bars, mean ± s.e.m.

After fear conditioning, mice displayed high levels of freezing to the CS^+ but not to the CS^- (CS^+: 48.96 ± 3.63 % versus CS^-: 12.91 ± 1.71 %) (Repeated Measures ANOVA, $F_{(1,14)}$ = 7.04, P = 0.019, **Fig. 3a**). In the HP session the temperature at which a nociceptive response was observed was significantly higher when the CS^+ was played compared with CS^- trial (HP_CS^+: 50.60 ± 0.42 °C versus HP_CS^-: 48.84 ± 0.67 °C) (Repeated Measures ANOVA, $F_{(1,14)}$ = 7.037, P < 0.05) (**Fig. 3b**). Likewise, the delay to observe a nociceptive response (**Fig. 3c**) during the CS^+ trial was significantly longer when compared to the CS^- trial (HP_CS^+: 209.86 ± 6.64 sec versus HP_CS^-: 191.99 ± 4.43 sec.) (Repeated Measures ANOVA, $F_{(1,14)}$ = 7.396, P = 0.0166). These results indicate that conditioned fear behaviour is associated with an *analgesia-like* effect when the CSs are played in the HP test.

In a second experiment the animals were subjected to a HP session in which the two trials were paired to the CS^- tone. The intent was to test the stability of the responses observed in the

HP (Δ Temp.) without the influence of fear conditioning (CS^+ is not played). The results (**Fig. 3d**) indicate that the average mean of temperature during the first and second presentation of the CS^- during the session was, respectively, 48.8 ºC (grey vertical line) and 49.3 ºC (blue vertical line). There was no significant difference between the two trials (Repeated Measures ANOVA, $P > 0.05$) indicating that nociceptive responses were stable over two distinct tests.

Experiment 1: Is the *analgesic-like* effect still visible when HP sessions are repeated?

Girardot et al. showed that repeated exposure to a stressful stimulus lead to a progressive decrease in stress-induces analgesia[26]. In addition, repeated HP tests with rats have been reported to change nociceptive response latencies. However, these results vary considerably between researchers[27–29]. Indeed, both Lai and Espejo laboratories have demonstrated that weekly, but not daily, repeated HP tests lead to changes in the nociceptive threshold, resulting in hyperalgesia[27,29]. In contrat, Gebhart and co-workers demonstrated that daily testing can also alter pain responses[28]. Hence, it would be interesting to test with our paradigm, if the *analgesic-like* behaviour is still visible after repeated HP testing sessions.

To address this issue, mice were submitted to the entire FCA procedure twice (**Fig. 4a**). The percentage of freezing behaviour during the fear retrieval test was evaluated for both tests (**Fig. 4b**). In both test 1 and in test 2 conditioned animals displayed significant difference between freezing levels during presentation of the CS^+ and CS^-, (test 1: CS^+: 54.90 ± 5.02 %, CS^-: 14.88 ± 2.51 %; Repeated Measures ANOVA, $F_{(2,14)}= 21.545$, $P < 0.001$ and test 2: CS^+: 49.05 ± 3.16 %, CS^-: 12.30 ± 3.05 %; Repeated Measures ANOVA, $F_{(2,14)}= 39.282$, $P < 0.001$). Importantly, there was no difference between the overall freezing levels observed in test 1 and test 2. Moreover, the CI was similar between the two tests (**Fig. 4c**, *Ps* > 0.05). Correlation analyses performed between the CI on tests 1 and 2 showed a positive correlation (i.e. higher fear levels in the first test correspond also to higher freezing levels in the second test) (**Fig. 4d**). This later point is important because it tells us that the animals maintained similar conditioned freezing levels during both retrieval tests. Therefore, any difference observed in the HP would result from the repetition of the HP test and not from differences in learning levels. As shown in **Figure 4e**, mice showed higher temperature response during the HP_CS^+ trials compared to HP_CS^- trials on both HP tests (*HP_CS^+ trial 1*: 50.55 ± 0.76 ºC and *HP_CS^+ trial 2*: 51.24 ± 0.34 ºC versus *HP_CS^- trial 1*: 49.24 ± 0.95 ºC and *HP_CS^- trial 2*: 49.75 ± 0.70 ºC). Our

analyses indeed confirmed that there was no effect of *session* (Repeated Measures ANOVA, P > 0.05) and no interaction between *session* and *CS factors*, yet there was an effect of the *CS* factor alone (Repeated Measures ANOVA, $F_{(1,7)}$ = 5.402 *P* = 0.0452) indicating that a comparable *analgesic-like* behaviour was observed in the two FCA tests.

a

	FC			HP	FC		HP
	Day 1: Hab.	Day 2: Cond.	Day 3: FR 1	Day 3: HP 1	Day 4: Cond. 2	Day 5: FR 2	Day 5: HP 2
CS+	4 CS	5 CS-US	4 CS	Cont. CS	5 CS-US	4 CS	Cont. CS
CS-	4 CS	5 CS	4 CS	Cont. CS	5 CS	4 CS	Cont. CS
↗ Temp.	-	-	-	√	-	-	√

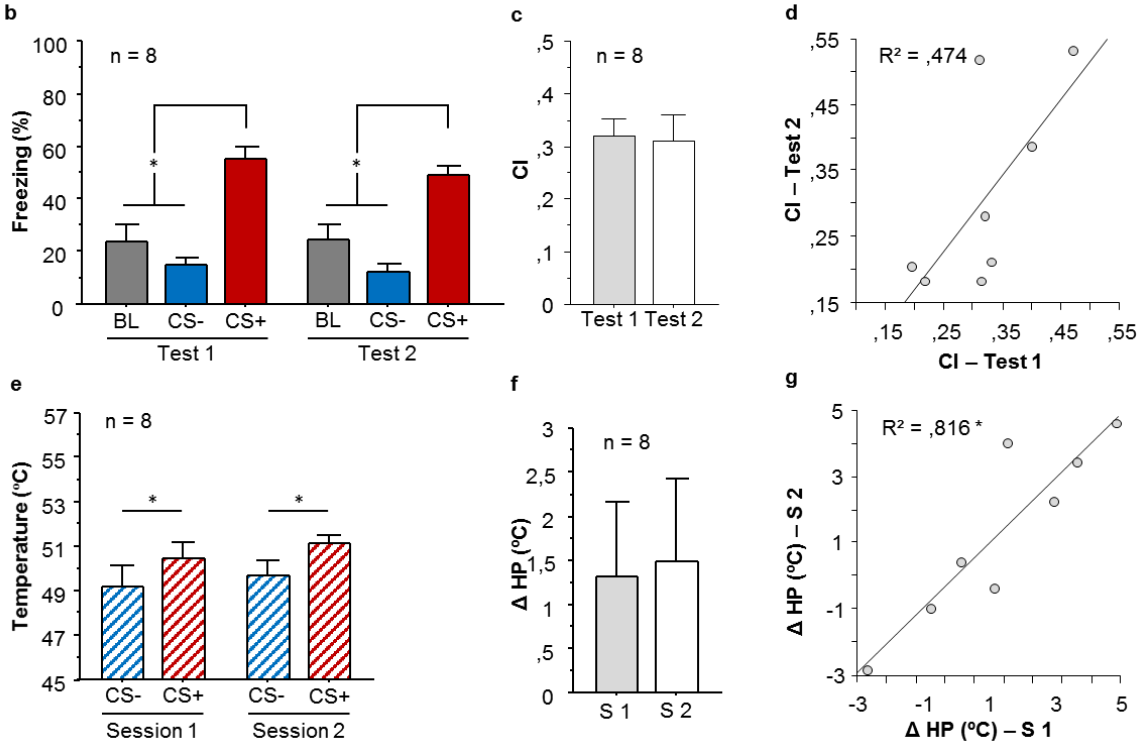

Figure 4 – Effect of repeating the HP session on *analgesia-like* behaviour. **a.** Behavioural Protocol. The animals were submitted to a fear conditioning protocol, which consists in an habituation session (Hab), a fear conditioning session (FC) and a fear retrieval session (FR). Afterwards a first HP session was done, followed by a second FR and HP. **b.** Mean percentage of freezing during the fear retrieval session. Mice (*n* = 8) exhibited high freezing states during the CS^+ but not for the baseline nor the CS^- presentations (Repeated Measures ANOVA, $F_{(2,14)}$ = 46229, *P* < 0,0001). Post-hoc Student-Newman-Keuls revealed significant differences between CS^+ and all other conditions. There were no significant difference between the mean percentage of freezing neither in test 1 and test 2 nor for the interaction between freezing percentage and test (Repeated Measures ANOVA, *Ps > 0.05*). **c.** Mean CI for the two fear retrieval tests. The levels of conditioning for both tests are statistically the same (Paired t-test, *P > 0.05*). **d.** Correlation between the conditioning index of test 1 and test 2. The conditioning index of the two tests is significantly correlated (R^2 = 0.474, *P* = 0, 0419). **e.** Mean temperatures for mice (*n* = 8) at which a *nociception-like* response was observed in the HP test. The analgesia effect was statistically significant for both HP sessions (Repeated measure ANOVA, $F_{(1,7)}$ = 5.402, *P* = 0,0452) and no difference were detected between the two tests nor for the interaction between the two factors (*Ps > 0.05*). **f.** Mean difference of temperature in both tests, which demonstrates that there are no significant differences between the two HP sessions (Paired t-test, *P > 0.05*). **g.** Correlation between the differences of temperatures in the first and the second hot-plate session. The difference of temperatures between both tests were significantly correlated (R^2 = 0816, *P* = 0,0021) Error bars, mean ± s.e.m.

In addition, the differences in temperature at which a nociceptive response was observed between the CS^+ and the CS^- during the HP test were also conserved between HP sessions. Moreover we observed a positive and significant correlation **(Fig. 4g)** between the differences in temperature during the two HP sessions confirming that analgesia can be observed across HP sessions (**Fig. 4f**). All together, these results indicate that the repetition of the HP tests does not alter the *analgesia-like* behaviour.

Experiment 2: Can the delay observed in the HP test be due to a change in the animal temperature?

The use of the HP test to assess FCA implies that the pain response observed during CS^+ trial occurs later than in CS^- trials, suggesting that the delay in response results from a decreased in pain sensitivity induced by the aversive valence of the CS^+. However, the use of a thermal nociception test in FCA has been reported to lead to possible erroneous interpretations because the fearful stimulus can lead to vasoconstriction in the tail and in the paws[5]. This could result from a redirection of the blood flow to the skeletal musculature, and thus to a decrease in the temperature in the extremities of the body which by itself could explain the delay observed for the nociceptive response during CS^+. Indeed, Vianna et al.[30] used infrared thermography to measure the body temperature during the 30 min period of re-exposure in a fear conditioned context and reported a decrease in skin temperature of -5.3 ^oC for the tail (from 31.6 to 26.3 ^oC) and -7.5 ^oC for the paws (from 34.8 ^oC to 27.3 ^oC), both forelimbs and hindlimbs. The authors clearly demonstrated a regionally specific response of skin vasoconstriction to aversive stimuli. Therefore, it is of the most importance to our project to understand if the delay latency observed during the HP_CS^+ is due to a decreased in pain sensitivity or to vasoconstriction. To evaluate this question we measured using a thermal camera, the temperature of the back and tail of the animals during CS^+ and CS^- presentations, without increasing the temperature of the HP. Similar temperature during HP_CS^+ and HP_CS^- would suggest that the FCA observed in the HP is due to pain modulation rather than a change in the animals temperature.

In this experiment the animals underwent a fear conditioning protocol followed by a HP test. The HP test consisted in two trials, in which one of the two tones were played without any changes in the temperature of the HP device. The animals were placed in the HP for a 60 s period of habituation to the apparatus followed by a *Pre-CS* period (130 s), the *CS* presentation (120 s)

and a *Post-CS* period (60 s) (**Fig. 5a**). The measure of the temperature of the back and tail of the mice was performed offline from the video acquired with the thermal camera. We made three distinct measures of the animal temperature in the back (**Fig. 5b, upper panel**) and in the tail **(Fig. 5b, lower panel)** from a video frame extracted every 30 s.

Figure 5 – Change in animal body temperature during HP. **a.** Protocol of the HP session. Mice were submitted to a 60 s

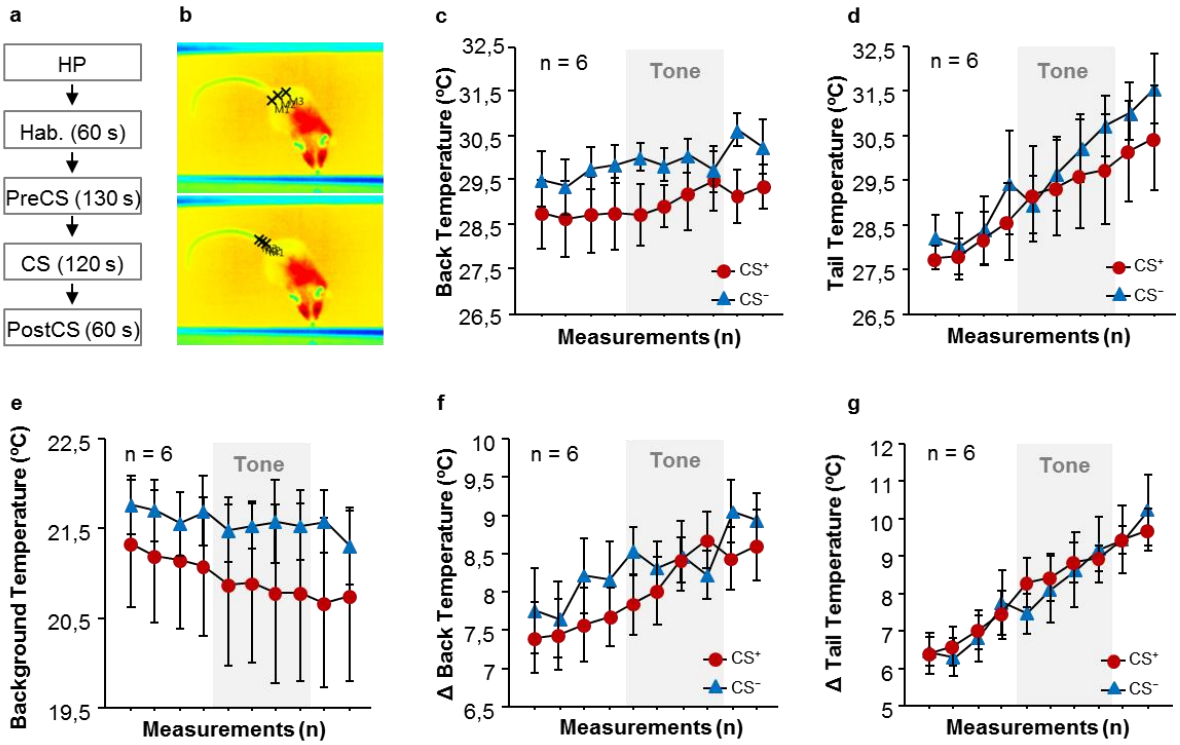

habituation period followed by a *Pre-CS* period (130 s), a *CS* period (120 s) and a *Post-CS* period (60 s). **b**. The animal body temperature was measured during the entire protocol in bins of 30 s. For each bin, three points in the animals' back (upper panel) and the tail (lower panel) were measured and averaged for each bin. **c.** Mean temperature of the animal's back (n = 6) during both the CS^- and the CS^+. There are no significant differences between the temperature measured during both CSs (Repeated Measures ANOVA, P > 0,05). **d.** Mean temperature of the animal's tail (n = 6) during the CS^- and the CS^+. There are no significant differences between the temperature measured during both CSs (Repeated Measures ANOVA, P > 0,05). **e.** Mean temperature of the background during both the CS^- and the CS^+. No significant differences between the temperature measured during both CSs were observed (Repeated Measures ANOVA, P > 0,05). **f.** Normalized mean variation of the temperature of the animal's back during CS^- and CS^+ presentations. There are no significant differences between the temperature of the CSs (Repeated Measures ANOVA, P > 0,05). **g.** Normalized mean variation of the temperature of the animal's back during CS^- and CS^+ presentations. There are no significant differences between the temperature of the CSs (Repeated Measures ANOVA, P > 0,05). Error bars, mean ± s.e.m.

Our results did not reveal any difference in body temperature between CS^+ and CS^- trials, neither in the back (**Fig. 5c**), nor in the tail (**Fig. 5d**) (*Ps* > 0.05). However, the results showed a substantial variability, which in part are caused by the sensitivity of the infrared digital thermographic camera. Thus, we normalized the results to the background (**Fig. 5e**). The background was the area outside the HP device that was also recorded by the infrared digital

thermographic camera. As such, after normalization, no difference was detected between the CSs, either in the back (**Fig. 5f**) or in the tail (**Fig. 5g**) of the animal (*Ps* > 0.05). Hence, we are confident that the delay response of the CS^+ during the HP test when compared to the CS^- in FCA (**Fig. 3 and 4**) is due to a decrease in pain sensitivity and not to variation of the animal temperature.

Experiment 3: What is the contribution of vlPAG SOM^+ interneurons in pain sensitivity?

In this set of experiments we first tested whether vlPAG SOM^+ interneurons play a role in pain sensitivity. We first evaluated the extent of SOM labelling within the vlPAG following viral injections (**Fig. 6**). Our results confirmed (i) the location of our injections in the vlPAG and (ii) the correct recombination of the AAV as illustrated with a clear GFP staining of vlPAG SOM^+ interneurons (**Fig. 6**).We next evaluated the effect of SOM^+ optogenetic activation on pain sensitivity in the HP test using several parameters as indicated in Table 1 in page 15.

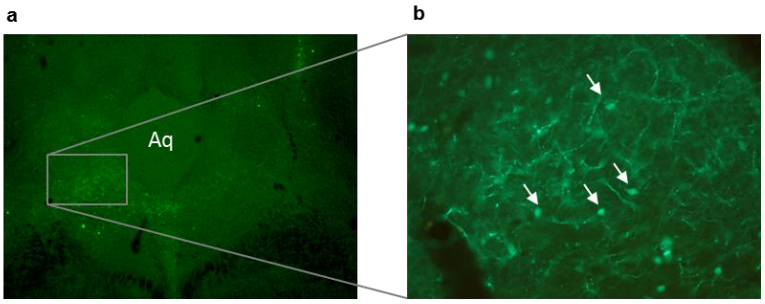

Figure 6 – Representative staining of SOM^+ interneurons. a. Magnification (4 X) of the mouse brain section infected with a cre-dependent AAV encoding for GFP and revealing the extent of the viral infection in the vlPAG (green labeling). **b.** Magnification (20 X) of the inset region in **(a)** which revealed the presence of GFP SOM^+ interneurons (arrows). Aq: Aqueduct.

Importantly, preliminary results collected in the laboratory indicated that under anaesthesia, the optimal optogenetic stimulation of SOM^+ in the vlPAG to increase pain sensitivity was achieved using either a 5 Hz stimulation (with a pulse of at 5 or 50 ms duration), or a 2 Hz stimulation (with a 5 ms pulse duration). Moreover, these preliminary results also revealed that an optogenetic activation of vlPAG SOM^+ interneurons transformed a tactile subliminal stimulus into a supraliminal stimulus (results not shown). As such, we decided to use the same strategy and parameters in behaving animals in which SOM^+ vlPAG interneurons were infected with ChR2 and that were submitted to a HP test session.

Our results show that using a 5 Hz stimulation and independently of the pulse duration used (**Fig. 7a-b**), the stimulated animals displayed a nociceptive response at a higher temperature compared to control animals (**Fig. 7a-b**) (test 5 Hz, 5 ms width, temperature during *Light* : 53.90 ± 0.75 °C versus *Control*: 51.07 ± 0.70 °C; test 5 Hz, 50 ms width, temperature during *Light* : 55.43 ± 0.79 °C versus *Control* : 51.68 ± 0.42 °C). Statistical analyses performed on these two experiments revealed significant differences between light and control conditions (test 5 Hz, 5 ms width, $t_{(8)} = 2.675$, $P = 0.0281$ (Unpaired t-test); test 5 Hz, 50 ms width, $t_{(8)} = 4.583$ $P = 0.0018$ (Unpaired t-test), suggesting that the optogenetic activation of vlPAG SOM^+ interneurons induces analgesia. This test was replicated two weeks later, showing that the effect was (data not shown) On the contrary, when tested with a 2 Hz frequency and a pulse width of 5 ms we observed a significant effect in the opposite direction, namely a nociceptive reaction for lower temperature under light conditions (**Fig. 7c**) (test 2Hz, 5 ms width, temperature during *Light*: 49.50 ± 0.33 °C versus *Control* : 51.43 ± 0.54 °C). These differences were moreover statistically significant (test 2 Hz, 5 ms width, $t_{(6)} = -3.048$, $P = 0.0226$ (Unpaired t-test)), indicative of a pro-nociceptive effect with a 2 Hz stimulation. As previously, a second test session was done with the same parameters in order to test the stability of this result: an equivalent pro-nociceptive effect was observed (data not shown).

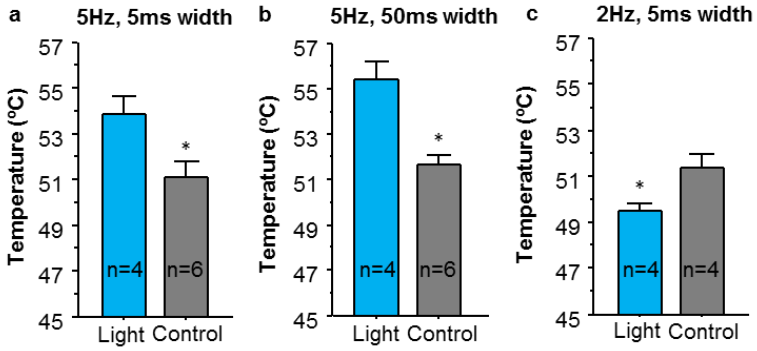

Figure 7 – Effect of the optogenetic activation of vlPAG SOM^+ interneurons in the HP test. a. Light stimulation with a pulse-duration of 5 ms at 5 Hz. There was a significant effect between the light ($n = 4$) and the control mice ($n = 6$) (Unpaired t-test, $t_{(8)} = 2.675$, $P = 0.0281$). The light stimulation leads to an *analgesia-like* effect as mice display a response at higher temperatures when compared to the control group. **b.** Light stimulation with a pulse-duration of 50 ms at 5 Hz**.**There was a significant difference in the temperature response between light ($n = 4$) and control animals ($n = 6$) (Unpaired t-test, $t_{(8)} = 4.583$, $P = 0.0018$), leading to a *analgesia-like* phenotype. **c.** Light stimulation with a pulse-duration of 5 ms at 2 Hz**.** There was a significant difference in the temperature response between light ($n = 4$) and control animals ($n = 4$)(Unpaired t-test, $t_{(6)} = -3.048$, $P = 0.0226$), leading to a *pronociceptive-like* phenotype. Error bars, mean ± s.e.m.

Together, these data clearly suggest an analgesic and pronociceptive effect with a 5 and 2 Hz stimulation frequency, respectively. However, an alternative explanation for the analgesic effect observed upon 5 Hz stimulation is the contribution of a motor effect of the stimulation that might prevent or delay the animals' response. To evaluate this possibility mice were submitted to an OF test during which vlPAG SOM$^+$ interneurons were stimulated at the frequency at which the *analgesia-like* phenotype was stronger (pulse of 50 ms length delivered at 5 Hz) (**Fig. 8a**). We simultaneously monitored whether or not the activation of vlPAG SOM$^+$ interneurons was associated with changes in locomotor activity. The analyses of the distance travelled during the pre-stimulation, stimulation and post-stimulation epochs reveals an *epoch* effect (Repeated Measures ANOVA, $F_{(2,19)} = 10.622$, $P = 0.0002$), but more interestingly, an interaction between *epoch* × *light* treatment factors (Repeated Measures ANOVA, $F_{(2,19)} = 3.674$, $P = 0.0348$). This result indicate that mice in which vlPAG SOM$^+$ interneurons were stimulated traveled less distance compared to the control conditions without light stimulation (**Fig. 8b**) (*Light, distance:* 230.93 ± 94.545 cm; *Control, distance:* 433.238 ± 68.358 cm), suggesting that vlPAG SOM$^+$ interneurons activation with a pulse of 50 ms length delivered at 5 Hz induces a decrease in motor activity.

We also analyzed whether there was a difference in the time spent in the center and in the periphery of the OF but no significant difference were observed ($P > 0.05$, data not shown), suggesting that the light stimulation *per se* does not alter the basal stress levels of the animals.

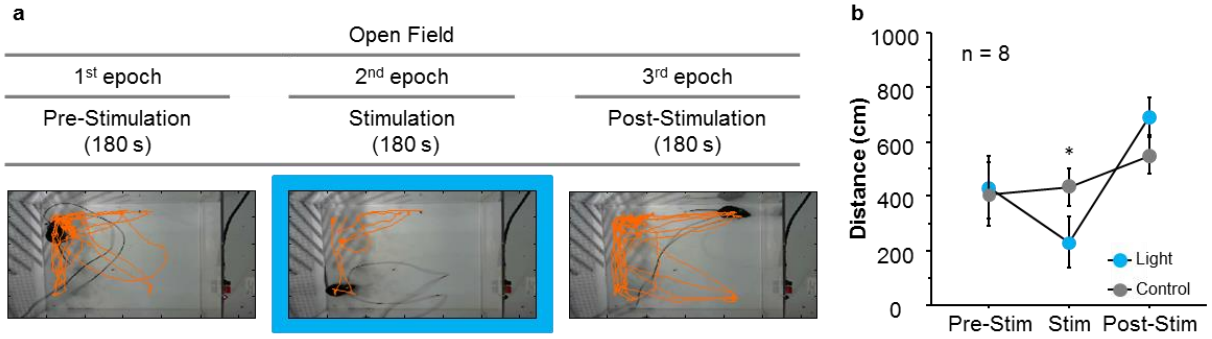

Figure 8 – Effect of vlPAG SOM$^+$ optogenetic activation on motor activity. a. Top, Protocol. The OF had three epochs each lasting 180 s. The epoch alternated between the light stimulation and no light stimulation trials, starting with the no light stimulation trial. For each trial, the first and the third epoch were considered as *Pre-* and *Post-Stimulation* epochs, respectively. The second epoch was the *Stimulation epoch.*. **Bottom**, Representative images of the offline tracking procedure to calculate the distances travelled. **b.** There was a significant effect in the distance traveled before, during and after the optical stimulation (Repeated measures ANOVA: $F_{(2,19)} = 10.622$, $P = 0.0002$). Post-hoc Student-Newman-Keuls revealed significant differences between the mean distance traveled after the light stimulation (*Post-Stim*) and the distance travelled before (*Pre-Stim*) and during the light stimulation (*Stim.*). During the stimulation period there was a significant difference between the *Control* and *Light treatment* ($F_{(2,19)} = 3.674$, $P = 0.0348$). Error bars, mean ± s.em.

Therefore, these data strongly suggest that the delay observed in the HP test is not due to an analgesic effect but rather to a motor effect. For instance, the activation of vlPAG SOM^+ interneurons could be painful by itself. In order to test whether the light activation of vlPAG SOM^+ interneurons has an aversive effect we performed the PP test (**Fig. 9a**). Our analyses indicate that infected mice did not displayed any place preference/avoidance after the optical stimulation of vlPAG SOM^+ interneurons when compared to baseline (when there was no light stimulation) (**Fig. 9b**, Repeated Measures ANOVA, $F_{(1,7)} = 2.300$, $P = 0.1732$; *Baseline trial:* 212.89. ± 25.22 sec. versus *Test trial:* 164.44 ± 26.796 sec.). Moreover, no significant effect was observed between mice that received *optical stimulation* and the *control* group ($P > 0.05$). This test was repeated 24 h later and the same outcome was observed (Ps > 0.05) (**Fig. 9c**), suggesting that at a pulse duration of 50 ms delivered at a frequency of 5 Hz is not aversive by itself.

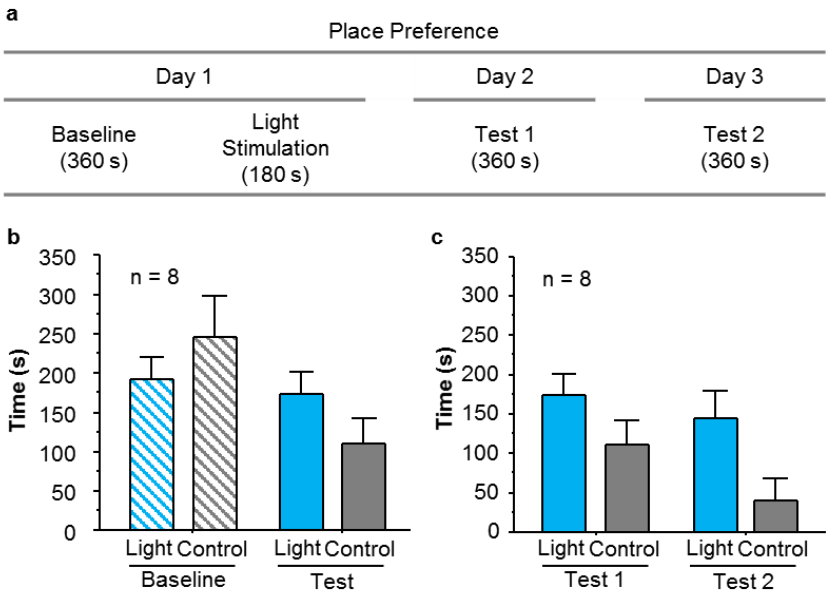

Figure 9 – Effect of optogenetic activation of vlPAG SOM^+ interneurons during the PP test. a. Protocol. On the first day two trials were performed, the *baseline trial* (without light stimulation) and the *light stimulation trial* (with light stimulation) (pulse-duration of 50 ms delivered at 5 Hz). On day 2 we performed the *test trial*, followed by another *test trial* the next day. **b.** There was no significant effect in the time spent in the chamber in which the animal received the stimulation between the *baseline trial* and the t*est trial* (Repeated Measures ANOVA, $F_{(1,7)} = 2.300$, $P = 0.1732$). Likewise, no significant differences was found between *Light* and *Control* animals (Repeated Measures ANOVA, $F_{(1,7)} = 0.139$, $P = 0.7200$). The stripes of the bars during the *baseline* trial demonstrate that no light stimulation was presented. Yet, the mice were group according to the *light treatment* that they would receive during the *light stimulation trial*. **c.** There was no significant effect in the time spent in the chamber in which the animal received the stimulation between the *test 1* and the *test 2* (Repeated Measures ANOVA, $F_{(1,7)} = 0.805$, $P = 0.3995$). Again, no significant differences was found between *Light* and *Control* animals (Repeated Measures ANOVA, $F_{(1,7)} = 4.279$, $P = 0.0774$). Error bars, mean ± s.e.m

Experiment 4: Are vlPAG SOM$^+$ interneurons involved/necessary for FCA?

Given the fact that with the 5 Hz at 50 ms width a strong locomotor effect was observed during the activation of the SOM$^+$ cells in the vlPAG, these parameters could not be used in the FCA. Therefore, we did several tests to find stimulation parameters that would not alter locomotion. We did not observe a change with a frequency of 5 Hz and pulse duration of 5 ms (data not shown). Hence, we used the 5 Hz at 5 ms width to test whether the vlPAG is involved in the *analgesic-like* behaviour observed in FCA (**Fig. 10a**).

a

	FC			HP
	Day 1: Hab.	Day 2: Cond.	Day 3: FR 1	Day 3: HP 1
CS+	4 CS	5 CS-US	4 CS	Cont. CS
CS-	4 CS	5 CS	4 CS	Cont. CS
↗ Temp.	-	-	-	√
Light	-	-	-	√

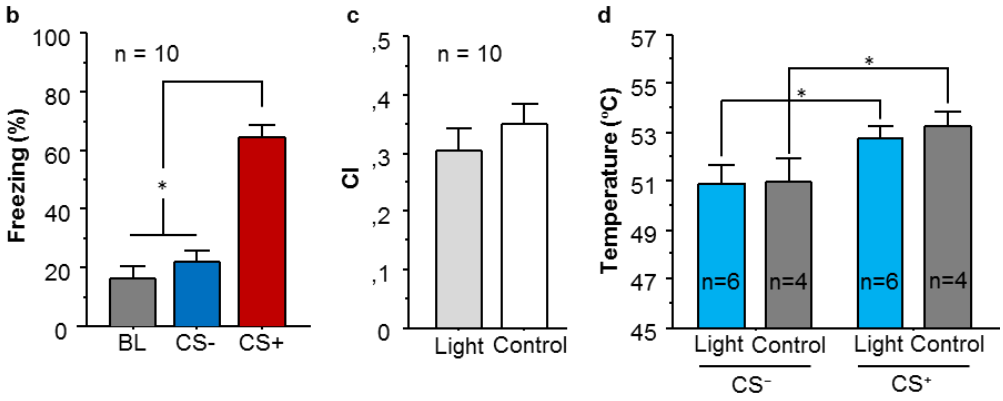

Figure 10 – Optogenetic manipulation of SOM$^+$ neurons in the vlPAG during FCA. a. Behavioural protocol. Mice were submitted to a fear conditioning protocol which comprised a habituation session (Hab), a fear conditioning session (FC), and a fear retrieval session (FR). If the mice were conditioned the HP was executed after the FR. **b.** Mean percentage of freezing observed in the fear retrieval. In the fear retrieval session mice (n = 10) exhibited a high freezing state for the CS$^+$ but not for the baseline nor the CS$^-$ (Repeated Measures ANOVA, $F_{2,18}$ = 163.011, P < 0.0001). Post-hoc Student-Newman-Keuls revealed significant differences between the freezing percentage of the CS$^+$ versus the baseline and CS$^-$. **c.** The CI for the fear retrieval failed to reveal any significant difference in freezing levels between the mice exposed to light stimulation and the control condition (Unpaired t-test, $t_{(8)}$ = -0.868, P = 0.4106). **d.** Mean temperatures for the *nociception-like* response in mice during the HP test. The analgesia effect was statistically significant for both groups independently of the light condition (Repeated measure ANOVA, $F_{1,8}$ = 8.118, P = 0.0215). Additionally, no significant differences were detected between the interaction of the light condition and the temperature in the HP test ($F_{1,8}$ = 0.070, P = 0.7975). Error bars, mean ± s.e.m.

In fear retrieval, freezing levels were significantly different (Repeated Measures ANOVA, $F_{2,18} = 163.011$, $P < 0.0001$). Post-hoc Student-Newman-Keuls revealed that the freezing levels during the fear retrieval was higher for the CS^+ when compared to both the freezing levels of the baseline and the CS^- (*CS^+:* 64.29 ± 4.36 % versus *baseline:* 16.60 ± 4.07 % and *CS^-:*22.13 ± 3.88 %) (**Fig. 10b**). The level of conditioning before the HP test was equivalent between controlled and light-stimulated animals, as shown in **Fig. 10c** by the CI ($P > 0.05$).

In the HP test, the *analgesia-like* behaviour was observed with a global *CS* effect (Repeated Measures ANOVA, $F_{1,8} = 8.118$, $P = 0.0215$), indicating that in both groups the CS^+ induces a delayed response in the HP (*HP_CS^+ Light*: 52.77 ± 0.51 °C and *HP_CS^+ Control*: 53.25± 0.57 °C versus *HP_CS^- Light*: 50.90± 0.76 °C and *HP_CS^- Control*: 51.00 ± 0.90 °C) (**Fig. 10d**). However, we did not observe any effect of the *optical stimulation* (Repeated Measured ANOVA, $F_{1,8} = 0.070$, $P = 0.7975$) suggesting that the analgesia effect observed with the activation of the SOM^+ cells in the vlPAG is suppress during the FCA, leading to no change in pain sensitivity upon fear modulation.

Experiment 5: What is the role of the PVa^+ cells in the vlPAG on pain sensitivity?

We did not evaluate the extent of PVa^+ cells labelling within the vlPAG following viral injections because these animals will be used in a future experiment.

Our results above indicate that activation of vlPAG SOM^+ interneurons using a stimulation of 5 Hz at 50 ms width during the HP lead to an *analgesic-like* effect, which in fact appeared to be due to a locomotor effect. Importantly, when activating the SOM^+ in vlPAG with the 5 Hz at 5 ms width in the HP test an *analgesic-like* effect was observed but no effect was observed with the same manipulation in FCA. Therefore the manipulation of vlPAG SOM^+ interneurons does not appear to be an efficient tool for evaluating the role of the vlPAG in FCA. As such we decided to manipulate another main class of inhibitory interneurons, PVa^+ interneurons. Keeping the same rational, in this set of experiments we wanted first to test whether PVa^+ neurons in the vlPAG play a role in pain sensitivity. Hence, we delivered ChR2 or ArchT in interneurons expressing PVa^+ and optically stimulate the neurons in the HP test without any auditory stimulation.

Our results indicate that with a pulse duration of 40 ms delivered at 20 Hz (**Fig. 11a, b**), there was a tendency for a pronociceptive effect as the stimulated animals infected with ChR2 in

vlPAG show a tendencies to produce a pain response at lower temperatures compared to control animals (test 1: ,temperature during *Light*: 50.80 ± 0.90 °C versus *Control*: 53.46 ± 0.75 °C; test 2: ,temperature during *Light*: 51.30 ± 0.80° C versus *Control*: 52.23 ± 0.46 °C). When combining the two tests, the *light* effect becomes significant (Unpaired t-test, $t_{(18)}$ = -2.413, *P* = 0.0267), indicating that the mice stimulated responded at lower temperatures when compared to the control (**Fig. 11c**) (temperature during *Light*: 51.05 ± 0.57 °C versus during *Control*: 52.74 ± 0.43 °C). These results suggest that the optogenetic activation of vlPAG PVa^+ interneurons induces an increase of pain sensitivity.

Interestingly, when inactivating vlPAG PVa^+ interneurons using ArchT, we observed a significant effect on the opposite direction (an analgesic effect) (**Fig. 11d**). Indeed, the mice which received light inhibition of vlPAG PVa^+ interneurons responded at higher temperatures when compared to control mice (temperature during *Light*: 52.97 ± 0.27 ºC versus *Control*: 51.22 ± 0.42 ºC) and this difference was statically significant (Unpaired t-test, $t_{(6)}$ = 2.969, P = 0.0250).

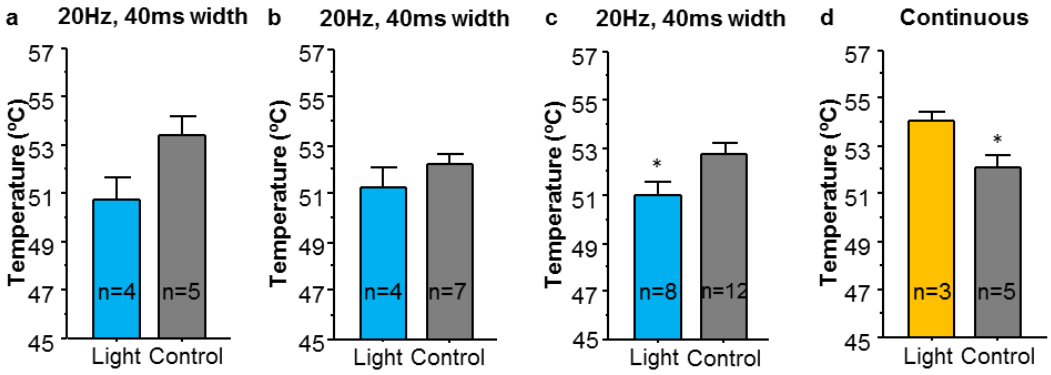

Figure 11 – Effect of optogenetic stimulation of vlPAG PVa^+ interneurons in HP test. a. Light stimulation with a pulse-duration of 40 ms, delivered at 20 Hz. There was a tendency for an effect between light (*n* = 4) and control mice (*n* = 5) (Unpaired t-test, $t_{(7)}$ = -2.296, *P* = 0.0553). **b.**The same parameters were used in a second batch of animals. There was no difference between light (*n* = 4) and control mice (*n* = 7) (Unpaired t-test, $t_{(9)}$ = -1.088, *P* = 0.3047). **c.** The two batch of mice were poolled and the effect of the *pronociceptive-like* effect became significant, mice (Light: *n* = 8; control: *n* = 12) displayed a pain response at lower temperatures when compared to the control group (Unpaired t-test, $t_{(18)}$ = -2.413, *P* = 0.0267). **d.** Continuous light inhibition of vlPAG PVa^+ interneurons. There was a significant effect in the temperature response in animals with light stimulation (*n* = 3) compared to control (*n* = 5) (Unpaired t-test, $t_{(7)}$ = 2.969, *P* =0.0250), leading to a *analgesia-like* phenotype. Error bars, mean ± s.e.m.

Since the inactivation of the vlPAG PVa^+ interneurons with ArchT in the HP test lead to a decrease in pain sensitivity, it is necessary to show that the light stimulation does not affect the animal motor activity. Therefore the animals were subjected to an OF test with continuous yellow light inhibition of vlPAG PVa^+ interneurons, to test whether the light inhibition of vlPAG PVa^+ interneurons had a locomotor effect (**Fig. 12a**). Our results demonstrated a significant difference

between the distance travelled during the three epochs (Repeated Measures ANOVA, $F_{(2,14)}$ = 6.437, P = 0.0050), suggesting that both groups show an increased activity within the session(**Fig. 12b**). However, we did not observed a *group* (Repeated Measures ANOVA, $F_{2,14}$ = 1.257, P = 0.2810), or *epoch* × *group* interaction (Repeated Measures ANOVA, $F_{2,14}$ = 2.044, P = 0.1484) (**Fig. 12b**) suggesting that the light inhibition of the PVa^+ neurons in the vlPAG *per se* does not affect the motor activity. Therefore, the *analgesia-like* effect observed during the HP test upon light inhibition ofvlPAG PVa^+ interneurons cannot be explained by a change in motor activity and is likely due to a decrease in pain sensitivity.

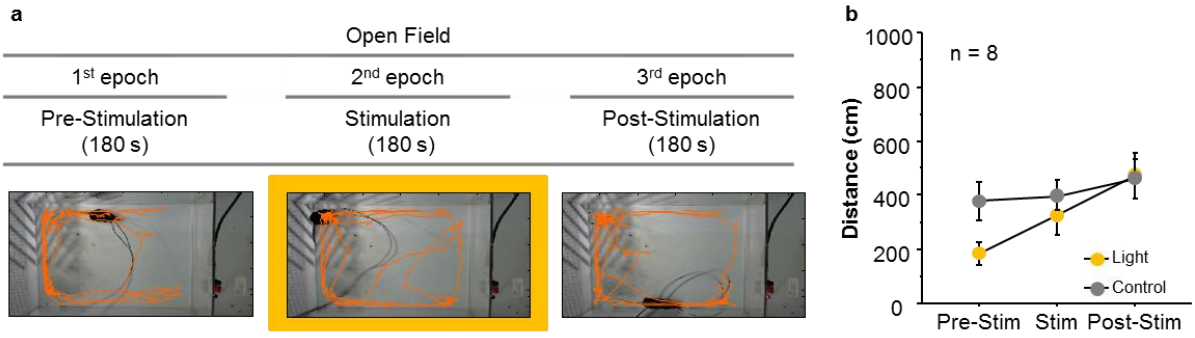

Figure 12 – Effect of optogenetic inhibition of vlPAG SOM^+ interneurons on motor activity. a. Top, Protocol. The OF had three epochs each lasting 180 s. The epoch alternated between the light stimulation and no light stimulation trials, starting with the no light stimulation trial. For each trial, the first and the third epoch were considered as *Pre-* and *Post-Stimulation* epochs, respectively. The second epoch was the *Stimulation epoch*. **Bottom**, Representative images of the offline tracking procedure to calculate the distances travelled. **b.** There was an overall significant effect in the distance travelled before, during and after the optical stimulation (Repeated Measures ANOVA, $F_{(2,\ 14)}$ = 6.437, *P* = 0.0050). Post-hoc Student-Newman-Keuls revealed significant differences between the mean distances traveled after the light stimulation (*Post-Stim*) and the Pre-Stim period. During the stimulation period there was no significant difference between *light* treatment (Repeated Measures ANOVA, $F_{(1,14)}$ = 1.257, *P* = 0.2810) nor for the interaction between the two factor (Repeated Measures ANOVA, $F_{(2,\ 14)}$ = 2.044, *P* = 0.1484). Error bars, mean ± s.e.m.

Experiment 6: Are the vlPAG PVa^+ interneurons involved/necessary for FCA?

Both group of animals used in the experiment above (ChR2 and ArchT-infected mice) were submitted to the FCA paradigm (**Fig. 13a**) In the fear retrieval test following conditioning, both groups were able to learn the CS-US association. Indeed, freezing levels were significantly different for both group of mice (ChR2: Repeated Measures ANOVA, $F_{2,18}$ = 143.889, P < 0.0001; ArchT, Repeated Measures ANOVA, $F_{2,18}$ = 46.849, P < 0.0001) (**Fig. 13 b,c**).

Post-hoc Student-Newman-Keuls revealed that freezing levels was higher during CS^+ compared to baseline and CS^- for both group of mice (ChR2: *CS^+:* 59.73 ± 0.88 % versus

baseline: 17.99 ± 3.68 % and *CS⁻:* 14.02 ± 2.276 %; ArchT : *CS⁺:* 69.93 ± 5.54 % versus *baseline:* 24.19 ± 4.003 % and *CS⁻:* 27.42 ± 4.33 %) (**Figure 13b, e**) As shown in **Figure 13c, f** the CI was equivalent between control and stimulated animals.

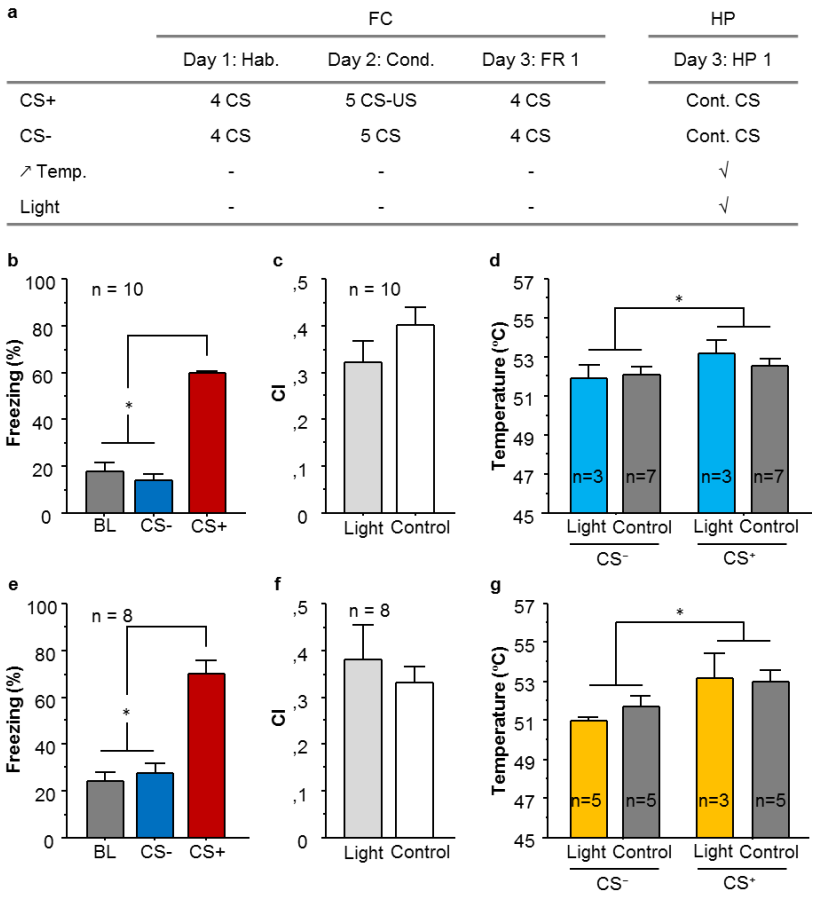

Figure 13 – Optogenetic manipulation of PVa⁺ neurons in the vlPAG during FCA. a. Behavioural protocol. Mice were submitted to a fear conditioning protocol, which comprised a habituation session (Hab), a fear conditioning session (FC), and a fear retrieval session (FR). If the mice were successfully conditioned, the HP test was performed after the FR. **b, e.** Mean percentage of freezing observed in the fear retrieval in mice infected with ChR2 **(b)** and ArchT **(e)**. In the fear retrieval session the two groups of mice **(b/e)** exhibited high freezing levels for the CS^+ compare to baseline and CS^- (ChR2, Repeated Measures ANOVA, $F_{2,18} = 143.889$, $P < 0.0001$; ArchT, Repeated Measures ANOVA, $F_{2,14} = 46.849$ $P < 0.0001$). Post-hoc Student-Newman-Keuls revealed significant differences between freezing levels during CS^+ versus baseline or CS^-. **c, f.** The CI for the fear retrieval test in mice infected with ChR2 **(c)** and ArchT **(f)** failed to reveal any significant difference in freezing levels for the mice exposed to light stimulation and the control condition (ChR2, Unpaired t-test, $t_{(8)} = -1.218$, $P = 0.2579$; ArchT, Unpaired t-test, $t_{(6)} = 0.692$, $P = 0.5150$). **d, g.** Mean temperatures for the *nociceptive-like* response in mice during the HP test. The analgesic effect was statistically significant for both the ChR2 group **(d)** (Repeated Measures ANOVA, $F_{1,8} = 6.038$, $P = 0.0395$) and the ArchT group **(g)** (Repeated Measures ANOVA, $F_{1,6} = 8.730$, $P = 0.0255$) independently of the light condition. Additionally, no significant differences were detected between the interaction of the light condition and the temperature in mice infected with ChR2 **(d)** (Repeated Measures ANOVA, $F_{1,8} = 1.534$, $P = 0.2506$) or ArchT **(g)** (Repeated Measures ANOVA, $F_{1,6} = 0.546$, $P = 0.4880$). Error bars, mean ± s.e.m.

Regarding mice infected with ChR2, in the HP test, the *analgesia-like* behaviour was observed with a global *CS* effect (Repeated Measures ANOVA, $F_{(1,8)} = 6.038$, $P = 0.0395$), indicating that in both groups the CS^+ induces a delayed response in the HP (*HP_CS*$^+$ Light: 52.20 ± 0.70^o C and *HP_CS*$^+$ *Control*: 52.57 ± 0.39 ^{o}C versus *HP_CS*$^-$ *Light*: 51.90 ± 0.70 ^{o}C and *HP_CS*$^-$ *Control*: 52.14 ± 0.35 ^{o}C) (**Figure 13d**). However, we did not observe any significant effect of the *optical stimulation* (Repeated Measured ANOVA, $F_{(1,8)} = 0.094$, P = 0.7665) nor the interaction between the factor *temperature* and *optical stimulation* (Repeated Measured ANOVA, $F_{1,8} = 1.534$, $P = 0.2506$). For mice infected with ArchT, in the HP test, the *analgesia-like* behaviour was also observed with a global *CS* effect (Repeated Measures ANOVA, $F_{(1,6)} = 68.730$, $P = 0.0395$), showing that in both groups the CS^+ leads to a higher temperature response in the HP (*HP_CS*$^+$ *Light*: 53.17 ± 1.27^o C and *HP_CS*$^+$ *Control*: 53.00 ± 0.57 °C versus *HP_CS*$^-$ *Light*: 51.00 ± 0.15 ^{o}C and *HP_CS*$^-$ *Control*: 51.70 ± 0.56 ^{o}C) (**Fig. 13g**). Similarly to the ChR2 group, we did not observe a significant effect of the *optical stimulation* (Repeated Measured ANOVA, $F_{(1,6)} = 0.108$, $P = 0.7537$) nor the interaction between the factor *temperature* and *optical stimulation* (Repeated Measured ANOVA, $F_{(1,6)} = 0.546$, P = 0.4880). Together these data indicate that the pro and antinociceptive effects observed for ChR2 and ArchT mice in the HP test, respectively were suppressed during the FCA test.

CHAPTER 4

DISCUSSION

4. Discussion

This study had two main objectives, the first one was to establish and validate the FCA paradigm in our laboratory. The second goal was to test the contribution of the vlPAG to FCA using state of the art, behavioral and optogenetic approaches. To do so, we combined Pavlovian auditory fear conditioning with a nociceptive thermal test (the HP test) in which we could investigate how an emotional component such as fear can influence a nociceptive response. The use of optogenetic tools allowed us to directly manipulate the vlPAG and investigate its contribution to pain processing and FCA.

Development and validation of the FCA paradigm

We first observed that in wild-type animals we could replicate the FCA paradigm developed in other laboratories. In particular we observed a higher temperature for pain responses in HP trials when the CS^+ was played compared to CS^- trials. This result suggests that the fear state induced by the CS^+ modulates the pain threshold exhibited by the animals in the HP test. Interestingly, in contrast to what has been reported by other authors such as Girardot et al. and Gebhart et al. [26,28], we did not found a change in the pain sensitivity during FCA after a second conditioning session and re-exposure to the HP test (**Fig.4**). The repetition of two HP sessions over two different days did not lead to a significant change in nociceptive responses and the FCA effect remained stable over time. One explanation for this difference with previous studies could rely on the test used to assess pain sensitivity. Indeed, Girardot el al. used intermittent cold water swims[26] and Gebhart et al used the HP test but with a fixed temperature[28] . Another explanation could come from the fact that the two above-mentioned studies used rats as subjects while we use mice. Nevertheless, because we did not find any influence of repetition on the FCA effect, we were able for subsequent experiments to test several time the same batch of animals in the HP.

Importantly, Vianna et al. reported that in a context previously associated with an aversive event, the animal temperature was changing while it was expressing fear[30]. More specifically, the authors observed a decrease in the body and tail temperature, which in our case could explain the delayed response observed in the HP test. Indeed, a tail or paw temperature decrease might delayed the pain response classically observed in the HP test .To verify whether or not the FCA effect could be explained by this phenomenon, we compared the temperature of the animals while playing the two CSs. Our results indicate that although both the tail and the back show an

increased temperature during the CSs, no difference was observed between CS^+ and CS^- trials (**Fig. 5)**. This result indicates that vasoconstriction and changes in the skin temperature induced by stress cannot explain the delayed response observed in the FCA test. It is important to note that Vianna et al. used a much longer time frame to evaluate changes in body temperature as animals were measure over a 30 min time period[30]. In contrast, our HP_CSs trial last a maximum of 3 min. This difference could explain that we did not observe any effect of CS on body temperature in our procedure. Thus, our results suggest that vasoconstriction plays a minor role if any, in the delayed response observed during HP_CS^+ trials.

Involvement of the vlPAG in FCA

Early studies in rats demonstrated that lesions to the PAG produced an alteration in the animals fear responses, for instance by blocking conditioned freezing behaviour [20,31–33]. In 1994 Bandler and Shipley characterized the PAG has having a columnar organization[34]. Thus, posterior studies (such as McDannald et al.[35]) could be more specific and target lesions the vlPAG which prevented freezing behaviour. More recently, Tovote et al. used an optogenetic approach in mice to light-activate $vGlut^{2+}$ excitatory neurons of the vlPAG, a manipulation which lead to an increase in freezing behaviour[21]. Moreover, in the same study the authors also demonstrated that the same manipulation in the vlPAG produced an analgesia effect as measured in the tail-flick test. These data strongly suggest that specific subpopulation of neurons within the vlPAG participate to both pain processing and fear behaviour. To manipulate the activity of the vlPAG and evaluate its contribution to pain processing and to the FCA effect, we used two different strategies based on the optogenetic manipulation of vlPAG inhibitory interneurons. In particular we performed an optogenetic manipulation of two main populations of interneurons expressing either somatostatin (SOM^+) or parvalbumin (PVa^+). These two interneuronal populations represent the two main populations observed in the cortex[36] and have also been described in the vlPAG[37–40].

We first tested the effect of the activation of the vlPAG SOM^+ interneurons on pain sensitivity (**Fig.7**). To do so, we used a stimulation of 5 Hz (with a pulse length of 5 or 50 ms), which induced a delayed response in the HP, which could be interpreted as analgesia. However subsequent control experiments (OF) indicated that the 5 Hz stimulation (with a light pulse of 50 ms) induced a drastic reduction of locomotor behaviour, a phenomenon not observed for the 5

Hz, 5 ms stimulation. The results are coherent with the literature describing the vlPAG as a key structure for the behavioural expression of freezing. In these studies, lesioning the PAG was associated with in an impairment in freezing behaviour. Moreover, in the vlPAG, freezing behaviour was dependent on the activation of $VGlut^{2+}$excitatory neurons projecting to the medulla[21]. Therefore, our results strongly suggest that the light-activation of vlPAG SOM^{+} interneurons induced a net disinhibition of vlPAG output neurons involved in freezing behaviour (**Fig.8**). Because freezing/immobility is likely to be a confounding factor for our results in pain sensitivity, we tried to dissociate the two behavioural outputs. We managed to do so using a stimulation frequency of 5 Hz with a 5 ms pulse width or using a 2 Hz stimulation. Interestingly, whereas we observed an *analgesic-like* effect with the 5 Hz, 5 ms stimulation, using a 2 Hz stimulation we observed a pro-nociceptive effect. The two opposite results seem difficult to reconcile although they could be related to the amount of inhibition induced by the two stimulations. This hypothesis would be consistent with the finding that as a function of the intensity, electrical stimulations of the PAG can have opposite behavioural effects[41,42]. Our results that the 5 Hz, 5 ms optogenetic stimulation of vlPAG SOM^{+} interneurons induced analgesia seems also in contradiction with the recent finding by Tovote et al., who reported that the light-activation of vlPAG $VGlut^{2+}$excitatory neurons projecting to the medulla leads to analgesia[21]. In the same line, lesion studies[43] suggest that the global activation of vlPAG leads to analgesia. However, a potential explanation of the apparent contradictory results would be that by activating vlPAG SOM+ interneurons we promoted a disinhibition of $VGlut^{2+}$excitatory neurons. The precise microcircuitry involved in the vlPAG would require further investigations. Finally, we did not observe any effect of the activation of vlPAG SOM^{+} interneurons (stimulation of 5 Hz, pulse width of 5 ms) on the FCA test.

In the time course of this project, we also evaluated the effect of the manipulation vlPAG PVa^{+} interneurons on pain sensitivity. When these interneurons where activated (ChR2), we observed a *pronociceptive-like* behaviour. On the contrary, if we inhibit these cells (ArchT) in the same test, we observe a delayed response in the HP, suggesting that this manipulation induces analgesia (**Fig. 11**). Importantly, we did not observe a change in motor activity when optically inhibiting the PVa^{+} interneurons. Hence, these results suggest that the inhibition of the PVa^{+} interneurons leads to a net activation of the vlPAG. The net activation of the vlPAG can be explained by a disinhibitory mechanism. Indeed, one potential explanation of these results is

vlPAG PVa^+ interneurons can contact principal neurons projecting to the medulla that will be disinhibited by the light-inhibition of PVa^+ interneurons, a phenomenon that could lead to analgesia. Finally, we did not observe any effect of the activation of vlPAG PVa^+ interneurons on the FCA test.

CHAPTER 5

CONCLUSION and FUTURE PERSPECTIVES

5. Conclusion and Future Perspectives

Conclusion

All together our results indicate that with the manipulation of vlPAG interneurons (SOM^+ and PVa+) we were unable to manipulate mice behaviour in the FCA paradigm, although we could systematically produce analgesia in the HP. One possible explanation of these results is that the FCA induces a stronger change in the network state compared to the potential effect of the optogenetic stimulation and therefore is counteracting the optogenetic manipulation on vlPAG interneurons. If this is the case, this would mean that the fear component overcomes the pain modulation that we observe in the HP test.

Future perspectives

Although our results are encouraging, several questions remain to be studied. The results gathered with the SOM-IRES-Cre mice need further investigation to fully understand the role of this population of interneurons in the vlPAG in pain modulation. More specifically, it would be interesting to investigate the effect of the inactivation of these cells in pain sensitivity. Our prediction will be that the inactivation of vlPAG SOM^+ interneurons promote an analgesic phenotype. Additionally, we plan to investigate the anatomy of the vlPAG microcircuits to identify the origin of the inputs received by these vlPAG SOM^+ interneurons using for instance recent retrograde transynaptic tracing rabies strategies[44]. The results obtained with the PVa^+ population in the HP are also promising, therefore in upcoming experiences one could decrease the level of conditioned fear. Indeed, reducing the strength of the fear modulation on pain could lead to a significant effect upon light-stimulation in the FCA test. Future studies should also investigate if the manipulation of the two populations of interneurons in the vlPAG can modulate fear responses using for instance optogenetic strategies.

CHAPTER 6

REFERENCES

6. References

1. Tovote, P., Fadok, J. P. & Lüthi, A. Neuronal circuits for fear and anxiety. *Nat. Rev. Neurosci.* **16,** 317–331 (2015).
2. LeDoux, J. E. Emotion Circuits in the Brain. *New York* **23,** 155–184 (2000).
3. Carrive, P. in *The midbrain periaqueductal Gray Matter* (eds. Depaulis, A. & Bandler, R.) 67–99 (1991).
4. Fanselow, M. S. The Midbrain Periaqueductal Gray as a Coordinator of Action in Response to Fear and Anxiety Functional Behavior Systems and Fear. *Midbrain Periaqueductal Gray Matter* 151–173 (1991). doi:10.1007/978-1-4615-3302-3_10
5. Butler, R. K. & Finn, D. P. Stress-induced analgesia. *Prog. Neurobiol.* **88,** 184–202 (2009).
6. Vogt, B. a. Pain and emotion interactions in subregions of the cingulate gyrus. *Nat. Rev. Neurosci.* **6,** 533–544 (2005).
7. Johansen, J. P., Tarpley, J. W., LeDoux, J. E. & Blair, H. T. Neural substrates for expectation-modulated fear learning in the amygdala and periaqueductal gray. *Nat. Neurosci.* **13,** 979–986 (2010).
8. Finn, D. P. *et al.* Behavioral, central monoaminergic and hypothalamo-pituitary-adrenal axis correlates of fear-conditioned analgesia in rats. *Neuroscience* **138,** 1309–1317 (2006).
9. Behbehani, M. M. Functional characteristics of the midbrain periaqueductal gray. *Prog. Neurobiol.* **46,** 575–605 (1995).
10. Bandler, R., Keay, K. a., Floyd, N. & Price, J. Central circuits mediating patterned autonomic activity during active vs. passive emotional coping. *Brain Res. Bull.* **53,** 95–104 (2000).
11. Keay, K. A. & Bandler, R. Parallel circuits mediating distinct emotional coping reactions to different types of stress. *Neurosci. Biobehav. Rev.* **25,** 669–678 (2001).
12. Lovick, T. a. Integrated activity of cardiovascular and pain regulatory systems: role in adaptive behavioural responses. *Prog. Neurobiol.* **40,** 631–644 (1993).
13. Keay, K. a. & Bandler, R. Parallel circuits mediating distinct emotional coping reactions to different types of stress. *Neurosci. Biobehav. Rev.* **25,** 669–678 (2001).
14. Carrive, P. The periaqueductal gray and defensive behavior : functional representation and neuronal organization. **58,** 27–47 (1993).
15. Depaulis, a, Keay, K. a & Bandler, R. Quiescence and hyporeactivity evoked by activation of cell bodies in the ventrolateral midbrain periaqueductal gray of the rat. *Exp. Brain Res.* **99,** 75–83 (1994).
16. Lewis, V. A. & Gebhart, G. F. Evaluation of the periaqueductal central gray (PAG) as a morphine-specific locus of action and examination of morphine-induced and stimulation-produced analgesia at coincident PAG loci. *Brain Res.* **124,** 283–303 (1977).
17. Yaksh, T. L., Yeung, J. C. & Rudy, T. a. Systematic examination in the rat of brain sites sensitive to the direct application of morphine: observation of differential effects within the periaqueductal gray. *Brain Res.* **114,** 83–103 (1976).
18. Kim, J. J., Rison, R. a & Fanselow, M. S. Effects of amygdala, hippocampus, and periaqueductal gray lesions on short- and long-term contextual fear. *Behav. Neurosci.* **107,** 1093–1098 (1993).
19. Walker, P. & Carrive, P. Role of ventrolateral periaqueductal gray neurons in the behavioral and cardiovascular responses to contextual conditioned fear and poststress recovery. *Neuroscience* **116,** 897–912 (2003).
20. LeDoux, J. E., Iwata, J., Cicchetti, P. & Reis, D. J. Different projections of the central amygdaloid nucleus mediate autonomic and behavioral correlates of conditioned fear. *J. Neurosci.* **8,** 2517–29 (1988).
21. Tovote, P., Esposito, M. S., Botta, P., Chaudun, F. & Jonathan, P. Midbrain circuits for defensive behaviour. *Nature, Press* (2016). doi:10.1038/nature17996
22. Helmstetter, F. J. & Landeira-Fernandez, J. Conditional hypoalgesia is attenuated by naltrexone applied to the

periaqueductal gray. *Brain Res.* **537,** 88–92 (1990).

23. Defrin, R. *et al.* Quantitative testing of pain perception in subjects with PTSD - Implications for the mechanism of the coexistence between PTSD and chronic pain. *Pain* **138,** 450–459 (2008).
24. Geuze, E. *et al.* Altered pain processing in veterans with posttraumatic stress disorder. *Arch. Gen. Psychiatry* **64,** 76–85 (2007).
25. Paxinos, G. & Franklin, K. *Paxinos and Franklin's the Mouse Brain in Stereotaxic Coordinates*. *São Paulo, Academic Press* (2012). at <https://www.elsevier.com/books/paxinos-and-franklins-the-mouse-brain-in-stereotaxic-coordinates/paxinos/978-0-12-391057-8>
26. Girardot, M. N. & Holloway, F. a. Effect of age and long-term stress experience on adaptation to stress analgesia in mature rats: role of opioids. *Behav Neurosci* **99,** 411–422 (1985).
27. Lai, Y. Y. & Chan, S. H. Shortened pain response time following repeated algesiometric tests in rats. *Physiol Behav* **28,** 1111–1113 (1982).
28. Gebhart, G. F., Sherman, A. D. & Mitchell, C. L. The Influence of Learning on Morphine Analgesia and Tolerance Development in Rats Tested on the Hot Plate. *Eur. J. Pharmacol.* **18,** 37–42 (1971).
29. Espejo, E. F. & Mir, D. Differential effects of weekly and daily exposure to the hot plate on the rat's behavior. *Physiol. Behav.* **55,** 1157–62 (1994).
30. Vianna, D. M. L. & Carrive, P. Changes in cutaneous and body temperature during and after conditioned fear to context in the rat. *Eur. J. Neurosci.* **21,** 2505–2512 (2005).
31. Lyon, M. The role of central midbrain structures in conditioned responding to aversive noise in the rat. *J. Comp. Neurol.* **122,** 407–429 (1964).
32. Liebman, J. M., Mayer, D. J. & Liebeskind, J. C. Mesencephalic central gray lesions and fear-motivated behavior in rats. *Brain Res.* **23,** 353–370 (1970).
33. Halpern, M. Effects of midbrain central gray matter lesions on escape-avoidance behavior in rats. *Physiol. Behav.* **3,** 171–178 (1968).
34. Bandler, R. & Shipley, M. T. Columnar organization in the midbrain periaqueductal gray: Modules for emotional expression? *Trends Neurosci.* **17,** 379–389 (1994).
35. McDannald, M. A. Contributions of the amygdala central nucleus and ventrolateral periaqueductal grey to freezing and instrumental suppression in Pavlovian fear conditioning. *Behav. Brain Res.* **211,** 111–117 (2010).
36. Ascoli, G. A. Petilla terminology: nomenclature of features of GABAergic interneurons of the cerebral cortex. *Nat. Rev. Neurosci.* **9,** (2008).
37. Johansson, O., Hökfelt, T. & Elde, R. P. Immunohistochemical distribution of somatostatin-like immunoreactivity in the central nervous system of the adult rat. *Neuroscience* **13,** 265–339 (1984).
38. Fehlmann, D. *et al.* Distribution and characterisation of somatostatin receptor mRNA and binding sites in the brain and periphery. *J. Physiol. Paris* **94,** 265–281 (2000).
39. Fu, W. *et al.* Chemical neuroanatomy of the dorsal raphe nucleus and adjacent structures of the mouse brain. *J. Comp. Neurol.* **518,** 3464–3494 (2010).
40. Taniguchi, H. *et al.* A Resource of Cre Driver Lines for Genetic Targeting of GABAergic Neurons in Cerebral Cortex. *Neuron* **71,** 995–1013 (2011).
41. Fardin, V., Oliveras, J. L. & Besson, J. M. A reinvestigation of the analgesic effects induced by stimulation of the periaqueductal gray matter in the rat. I. The production of behavioral side effects together with analgesia. *Brain Res.* **306,** 105–123 (1984).
42. Fardin, V., Oliveras, J. L. & Besson, J. M. A reinvestigation of the analgesic effects induced by stimulation of the

periaqueductal gray matter in the rat. II. Differential characteristics of the analgesia induced by ventral and dorsal PAG stimulation. *Brain Res.* **306,** 125–139 (1984).

43. Helmstetter, F. J. & Tershner, S. A. Lesions of the Periaqueductal Medulla Disrupt Antinociceptive Conditional Responses Gray and Rostra1 Ventromedial but Not Cardiovascular Aversive. **14,** (1994).
44. Callaway, E. M. & Luo, L. Monosynaptic Circuit Tracing with Glycoprotein-Deleted Rabies Viruses. *J. Neurosci.* **35,** 8979–8985 (2015).
45. Fenno, L., Yizhar, O. & Deisseroth, K. The Development and Application of Optogenetics. *Annu. Rev. Biomed. Eng.* **34,** 389–412 (2011).
46. Dugué, G. P., Akemann, W. & Knöpfel, T. A comprehensive concept of optogenetics. *Prog. Brain Res.* **196,** 1–28 (2012).
47. Deisseroth, K. Optogenetics. *Nat. Methods* **8,** 26–29 (2011).
48. Zhang, F. *et al.* Optogenetic interrogation of neural circuits : technology for probing mammalian brain structures. *Nat. Protoc.* **5,** 439–456 (2010).
49. Belzung, C., Turiault, M. & Griebel, G. Optogenetics to study the circuits of fear- and depression-like behaviors: A critical analysis. *Pharmacol. Biochem. Behav.* (2014). doi:10.1016/j.pbb.2014.04.002
50. Yizhar, O., Fenno, L. E., Davidson, T. J., Mogri, M. & Deisseroth, K. Optogenetics in Neural Systems. *Neuron* **71,** 9–34 (2011).
51. Zhang, F. *et al.* The Microbial Opsin Family of Optogenetic Tools. *Cell* **147,** 1446–1457 (2011).
52. Boyden, E. S., Zhang, F., Bamberg, E., Nagel, G. & Deisseroth, K. Millisecond-timescale , genetically targeted optical control of neural activity. *Nat. Neurosci.* **8,** 1263–1268 (2005).
53. Zhang, F., Wang, L., Boyden, E. S. & Deisseroth, K. Channelrhodopsin-2 and optical control of excitable cells. *Nat. Methods* **3,** 785–792 (2006).
54. Deisseroth, K. *et al.* Next-Generation Optical Technologies for Illuminating Genetically Targeted Brain Circuits. *J. Neurosci.* **26,** 10380–10386 (2006).
55. Tye, K. M. & Deisseroth, K. Optogenetic investigation of neural circuits underlying brain disease in animal models. *Nat. Neurosci.* **13,** (2012).
56. Warden, M. R., Cardin, J. A. & Deisseroth, K. Optical Neural Interfaces. *Annu. Rev. Biomed. Eng.* **16,** 103–129 (2014).
57. Häusser, M. Optogenetics : the age of light. *Nat. Publ. Gr.* **11,** 1012–1014 (2014).
58. Deisseroth, K. Optogenetics : 10 years of microbial opsins in neuroscience. *Nat. Neurosci.* **18,** 1213–1225 (2015).
59. Nagel, G. *et al.* Channelrhodopsin-2, a directly light-gated cation-selective membrane channel. *PNAS* **100,** 13940–13945 (2003).
60. Rein, M. L. & Deussing, J. M. The optogenetic (r) evolution. *Mol Genet Genomics* **287,** 95–109 (2012).
61. Kato, H. E. *et al.* Crystal structure of the channelrhodopsin light-gated cation channel. *Nature* (2012). doi:10.1038/nature10870
62. Han, X. *et al.* A high-light sensitivity optical neural silencer: development and application to optogenetic control of non-human primate cortex. *Front. Syst. Neurosci.* **5,** 18 (2011).
63. Raimondo, J. V, Kay, L. & Ellender, T. J. Optogenetic silencing strategies differ in their effects on inhibitory synaptic transmission. *Nat. Neurosci.* **15,** 1102–1104 (2012).
64. Sakaguchi, M. *et al.* Inhibiting the Activity of CA1 Hippocampal Neurons Prevents the Recall of Contextual Fear Memory in Inducible ArchT Transgenic Mice. *PLoS One* **10,** e0130163 (2015).
65. Taniguchi, H. Genetic dissection of GABAergic neural circuits in mouse neocortex. *Front. Cell. Neurosci.* **8,** 1–22 (2014).

66. Wolff, S. B. E. *et al.* Amygdala interneuron subtypes control fear learning through disinhibition. *Nature* **509,** 453–458 (2014).
67. Taniguchi, H. Genetic dissection of GABAergic neural circuits in mouse neocortex. *Front. Cell. Neurosci.* **8,** 1–22 (2014).
68. Pala, A. & Petersen, C. C. H. In Vivo Measurement of Cell-Type-Specific Synaptic Connectivity and Synaptic Transmission in Layer 2/3 Mouse Barrel Cortex. *Neuron* **85,** 68–75 (2015).
69. Xu, H., Jeong, H.-Y., Tremblay, R. & Rudy, B. Neocortical somatostatin-expressing GABAergic interneurons disinhibit the thalamorecipient layer 4. *Neuron* **77,** 155–67 (2013).
70. Kvitsiani, D. *et al.* Distinct behavioural and network correlates of two interneuron types in prefrontal cortex. *Nature* **498,** 363–366 (2013).
71. Chen, S. X., Kim, A. N., Peters, A. J. & Komiyama, T. Subtype-specific plasticity of inhibitory circuits in motor cortex during motor learning. *Nat. Neurosci.* **18,** 1109–1115 (2015).
72. Kang, S. J. *et al.* Bidirectional modulation of hyperalgesia via the specific control of excitatory and inhibitory neuronal activity in the ACC. *Mol. Brain* **8,** 81 (2015).
73. Cottam, J. C. H., Smith, S. L. & Hausser, M. Target-Specific Effects of Somatostatin-Expressing Interneurons on Neocortical Visual Processing. *J. Neurosci.* **33,** 19567–19578 (2013).
74. The Jackson Laboratory. at <https://www.jax.org/>
75. Wolff, S. B. E. *et al.* Amygdala interneuron subtypes control fear learning through disinhibition. *Nature* **509,** 453–458 (2014).
76. Hu, H., Gan, J. & Jonas, P. Interneurons. Fast-spiking, parvalbumin^{+} GABAergic interneurons: from cellular design to microcircuit function. *Science* **345,** 1255263 (2014).
77. Shang, C. *et al.* A parvalbumin-positive excitatory visual pathway to trigger fear responses in mice. *Science (80-.).* **348,** 1472–1477 (2015).
78. Courtin, J. *et al.* Prefrontal parvalbumin interneurons shape neuronal activity to drive fear expression. *Nature* **505,** 92–6 (2014).
79. Ledri, M., Madsen, M. G., Nikitidou, L., Kirik, D. & Kokaia, M. Global Optogenetic Activation of Inhibitory Interneurons during Epileptiform Activity. *J. Neurosci.* **34,** 3364–3377 (2014).

CHAPTER 7

SUPPLEMENTARY INFORMATION

7. Supplementary information

Optogenetics

Historical perspective

The need of a technique that would allow for manipulation of specific types of cells arise early in neuroscience, Crick in 1979 mentioned that "a method by which all neurons of just one type could be inactivated, leaving the other more or less unaltered"[45]. Twenty years later Crick went further, suggesting that "one of the next requirements is to be able to turn the firing of one or more types of neuron on and off in the alert animal in a rapid manner. The ideal signal would be light, probably at an infrared wavelength to allow the light to penetrate far enough."[46] Many years passed until an approach that comprised the need for control of specific events in specific cell types at defined times in intact systems, both *in vitro* and *in vivo,* arise. Not until 2010 this problem was solved, were optogenetics was introduced by Deisseroth[47] as "the combination of genetic and optical methods to achieve gain or loss of function of well-defined events in specific cells or living tissue".

Experimental design considerations

Before the emergence of optogenetics, high-temporal and cellular precision within intact neuronal tissue was not able to be achieve with one single technique. Extracellular electrical manipulation although having the temporal precision, lack the cell type specificity since in addition of the targets cells, it can simultaneously modify the surrounding cells and the passing axonal fibers[45,48]. On the other hand, pharmacological and genetic manipulations can give cell type specificity within a given population but lack temporal precision on timescale relevant to physiological conditions because of the slow kinetics and poor reversibility[45,48]. Therefore, optogenetics is a noninvasive technique that can pass by the above mentioned problems in the sense that it is able to control the activity of a given cell type within a heterogeneous population with high temporal precision at physiological rates and rapid deactivation upon cessation of light stimulation[48,49]. These properties must be able to sustain even in systems as complex as freely moving animals[45].

In addition, it is important to note that optogenetics is not just optical excitation and/or inhibition of the target cells, it has to be gain and loss of function of a precise event under control in order to prove causality and necessity[50]. In optogenetics, the gain of function demonstrates that the pattern of activity in the target population is causally sufficient for a given property. However, this does not excluded the fact that other neuronal populations might encode for the same circuit or behavioural property. As such, loss of function establishes the necessity of activity in the target population[50]. Once necessity and sufficiency is established, one can claim to demonstrate causal relationship.

Opsin Proteins – Type I and Type II

In order to manipulate cells thru light with high specificity and temporal precision a major class of light-sensitive proteins are widespread used in this field of research, the opsin proteins. The opsin proteins are a family of seven transmembrane helix (TM), light-responsive encoded by opsin genes[51]. The opsin genes are divided into two families: microbial opsins (type I) and animal opsins (type II)[45,51]. Both types of proteins bound to a cofactor, a vitamin-A related organic molecule called retinal, required to absorb photons. When the protein and the cofactor are covalently bound, the functional opsin is named rhodopsin[45,50]. The amino acid residues of the opsin protein in the binding pocket defines the ionic environment of the protonated retinal Schiff base (RSB+) once the retinal binds to it, and this predicts the spectral and kinetic characteristics of each opsin protein[45].

Type II opsin genes are present in higher eukaryotes, being mainly responsible for vision yet also having a role in circadian rhythm and pigmentation[51]. These opsins genes encode for G-protein-coupled receptors (GPCRs) and are bind to retinal in an 11-*cis* configuration. Upon illumination the 11-*cis* retinal isomerizes to the all-*trans* configuration, leading to phototransduction second messenger signaling cascade[45,51]. After isomerization the all-*trans* retinal dissociates from the opsin, requiring the recruitment of a new 11-*cis* retinal molecule[51].

Type I opsin genes are found in prokaryotes, algae and fungi and control diverse functions related to the ecology of the organisms, such as phototaxis or energy storage[51]. These opsin gene encode for proteins that bind to retinal in an all-*trans* configuration, which isomerizes into the 13-*cis* configuration upon photo absorption. However, in these type of opsins the retinal does not dissociate from the protein, instead it thermally reverts to the all-*trans* configuration thus

maintaining the covalent bond[45,51]. This reversible reaction, unlike in type I opsin, allows for a rapid kinetics that is essential for the use of microbial rhodopsins to modulate neuronal activity at high frequencies when used in optogenetics.

Single-Component Tools

In 2005 Boyden and co-workers reported that introduction of a microbial opsin gene into mammalian neurons lead to a reliable sustained control of millisecond-precision action potentials[52]. Additionally, these and other reports found out that mature mammalian brains and other vertebrates tissues contain enough all-trans retinal for expression of the microbial opsin genes in order to constitute a single-component system[52–54].

The microbial opsin proteins are nowadays common optogenetics tools, currently a great variety of classes of the rhodopsins can be found at the disposal of researcher. The rhodopsins can be divided in four major classes of single-component optogenetics tools (**Supplementary Fig.1**).

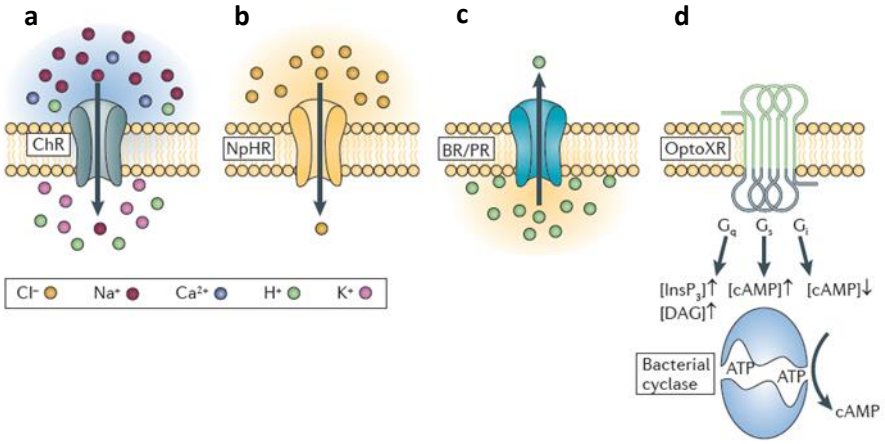

Supplementary Figure 1 – Major classes of single-component optogenetics tools. a. Cation-permeable channels for membrane depolarization, such as channelrhodopsins (ChRs). **b.** Chloride pumps, as halorhodopsin (NpRH) or archaerhodopsin (Arch) for membrane hyperpolarization. **c.** Proton pupms, for example bacteriorhodopsin (BR), as the previous, also for membrane hyperpolarization. **d.** light-activated membrane-bound G protein-coupled (OptoXR) or soluble (bacterial cyclase) receptors that mimic signaling cascades. Adapted from Tye et al., 2012.

The size, kinetic properties and wavelength sensitivity of photocurrents differ greatly within the different classes. Moreover, new experimental designs and the more powerful and refined manipulations are given rise to new engineered variants of opsins[50,55]. These experimental manipulations target the physiologic effect, the kinetic properties and the wavelength, the power

and spatial extent of light signal. With the available single-component optogenetic tools it is now possible not only to do fast excitation and inhibition but also to do bistable modulation and control of intracellular signaling cascades[50,55]. The specific characteristics of each class of rhodopsin in beyond the scope of our project and therefore will not be reviewed. Further ahead, more detailed information will be given regarding the two rhodopsins used in this project, ChR2 and ArchT.

Opsin Gene Delivering

One of the strategies widely used for targeting the opsin genes for cell-type specific expression is through viral expression systems. Viral vector based on lentivius and adeno-associated virus (AAV) associated with a promotor are very common, providing cell-type specificity and stable long-term and high levels of protein expression[46]. Still, the virus have limited packing capacity (< 10 kb for lentivirus and < 5 kb for AAV), preventing the use of large promotor fragments and thus compromising the specificity, since small, specific and strong promoters are rare[45,48,49]. Additionally, the levels of opsin gene expression are not homogeneous across the transduced cells and some cell type-specific promotors do not have strong expression levels of the downstream gene[48,49].

Given the limitations stated above, another approach involves the use of mouse Cre-driver lines. The cell-specificity is given by the enzyme Cre-recombinase expression, thus the DNA does not have to be packed inside the virus particle, allowing for a greater specificity than with the viral system[48,49]. The spatial accuracy and strong expression is reached with stereotaxic injection of the virus inclosing a conditional allele of the opsin gene of interest behind a strong ubiquitous promotor[48,49]. This technique was improved with the doublefloxed inverted open-reading frame (DIO)[45] (**Supplementary Fig. 2**). In this system, the opsin gene is inverted and positioned between two sets of incompatible Cre recombinase recognition sequences. In the Cre expressing cells the recombination of the viral DNA lead to the reversal of the opsin gene and set the open reading frame behind the strong promoter[45].

Although the Cre-dependent optogenetic system has many advantages it has also some limitations that one must keep in mind while designing the experiments. The infection efficiency is not spatially homogeneous, which means that the expression decreases away from the injection site. Also, the targeted cells might not express the same amount of opsin protein[46]. Another

potential limitation is toxicity due to the high transcription rates that lead to toxic accumulation of the opsin protein[46].

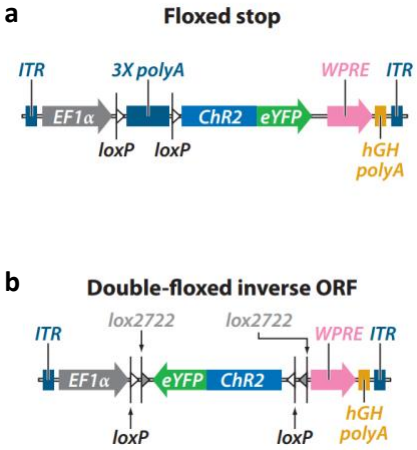

Supplementary Figure 2 – Comparison between DIO and lox-flox-lox strategy. In the absence of Cre recombinase, in the DIO strategy because the ORF of an opsin encodes nonsense there is no functional expression. Adapted from Fenno et al. 2011

Light Delivery

Light delivery for optogenetic control of neuronal activity is utmost importance, supplying light at a sufficient intensity to a define target area without getting out of the physiological context is the aim in optogenetics. The light delivery system to activate rhodopsins must control the rate of absorption of photons of a given wavelength, which is proportional to the local photon flux[50]. However, it is common to refer to light power density rather than photon flux. Light power density is the photon flux multiplied by the energy of the individual photon, thus typically measured in mW/mm^2 [50]. The light power density requirements depends on the tools and on the single-component molecule. For example, for photostimulation to control the neuronal firing 1-5 mW/mm^2 is sufficient[56]. In order to estimate the light power density one needs to have in account the propagation of light in tissue[50]. Light propagation in biological systems depends on the degree of light scattering and the absorption by the target tissue, for that mathematical models are available to determine the parameters for experimental configuration [56]. To deliver light in deep brain areas there is a need for optical fibers. Optical fibers are thin, flexible cables made of transparent material that guide the light to deep brain areas without damaging the surrounding tissue[50]. In addition, the length of the bare optical fiber can be adjust based on the target brain area[48]. For freely behaving animals it is custom to use chronic implanted optical fibers. Significant advantages comes with this strategy, namely avoidance of repeated insertion and

thereby reducing tissue damage, reducing the probability of breaking the fiber upon insertion into the brain and reducing the handling stress for the animal[56]. Note that the light coming out of the optical fiber is emitted in a conical pattern, getting scattered and absorbed as it passes through the tissue. Mammalian brain tissue scatters light greatly, with only 10% of the initial light power density reaching the target area at a distance from the fiber tip of approximately 500 μm[48]. Therefore, this is something that the researcher should be aware when defining the light delivery parameters. The light source for the optical fiber can be either laser or light-emitting diode (LED). Laser source can be easy manipulated and focused into the fiber core (low beam divergence) while LEDs are cheaper and available in a great range of waveforms but with lower coupling efficiency[46,56].

Limitations and experimental considerations

Despite the outstanding advance that optogenetics have given to the field of neuroscience there are several limitations that are important to know when using optogenetics. For instance, when doing photoexcitation, the level of stimulation may be outside the physiological range which, unless doing electrical recordings simultaneously, may be particularly difficult to evaluate. If such, this can lead to downstream effects that would not occur under physiological conditions[57]. Another concern is the precise synchronized stimulation of the target population, possibly leading to unphysiological activity since in mammalian neuronal circuits it is rare to find population of neurons with synchronized activity[57]. Light stimulation might also lead to antidromic stimulation thus inducing numerous indirect side effects, potentially leading to confounded results[49,57].

One caveat important to also mention is toxicity. Long-term and/or very high-levels membrane protein overexpression can lead to toxicity, therefore no-light controls in opsin-expressing systems, in which there is viral transduction but no light delivered, can assess if there is toxicity[50].

Another control necessary is the no-opsin control, where identical light parameters are used in a virally non-transduced target, this would allow to control possible photodamage or local temperature increases from the light itself that might altered the outcome[58]. Furthermore, each optogenetic experiment should include histological validation, as well as baseline comparisons within the different conditions[58].

Channelrhodopsin 2

ChR2 is naturally found *in Chlamydomanas reinhardtii*, being confined to the pigmented eyespot region, generating photocurrents in these green algae[59]. ChR2 is a light-gated cation channel that opens upon illumination of blue light (maximally activated at 470 nm) leading to a passive influx of mainly Na^+ and, to minor extent Ca^{2+} ions, along the membrane gradient, giving rise to the depolarization of the cell membrane in the cells expressing this rhodopsin[60]. It consists of 737 amino acids and the photocurrent functionality is containing in the approximately 300 amino acids of the amino-terminal[61]. The channel of this protein, despite having low selectively to cations, does not conduct anions, thus being a selective channel[59]. Regarding the cations, it is know that the selectively filter is larger than that of a voltage-activated Na^+ channel and that the light-activated conductance for Na^+ is inward rectifying, being evoked within 50 µs after a flash of blue light[59]. In addition, the selectively filter is mediated by the electronegative pore that is formed by the transmembrane domains 1, 2, 3 and 7. Since most of the negatively charged amino residues are derived from TM2, this suggested that the ion conductance and the selectively of ChR2 is mediated the TM2[61].

Nagel and co/workers showed in 2003 that ChR2 could be expressed in oocytes of *Xenopus laevis* and mammalian cells, functioning as a light-gated cation-selective membrane channel. In 2005 it was demonstrated that the ChR2 could be expressed in mammalian neurons, driving depolarization. Moreover, the same researched showed that ChR2 was able to sustainable mediate large-amplitude photocurrents within millisecond-timescale control with the rapid activation kinetics (deactivation time constant ≈ 12 ms) [48,52]. Importantly, the mediate neuronal spiking was achieved within a physiologically relevant range of firing frequencies and no significant changes in cell health or basal electrical properties of the expressing neurons were detected[52].

ArchT

This light-driven proton pump derived from the halobacteria *Halorubrum* sp. TP009 was reported in 2011 by Han and co-workers as being expressed in the membrane of mammalian neurons resulting in neuronal silencing[62]. The use of the light-driven outward proton pumps have several advantages over the other type of neuronal silencers, the inward chloride transporters (NpHR). For instance, the NpHR, unlike ArchT, leads to accumulation in intracellular Cl^- which

results in changes in the reversal potential of the $GABA_A$ receptors thus resulting in changes in synaptically evoked spiking activity in the after the cessation of an extend period of photon-activation[63,64]. In fact, it was demonstrated that silencing neuronal activity with a Cl^- pump, but not H^+ pump, alters the GABaergic synaptic transmission beyond the period of silencing and in a manner that alters the network excitability[63].

ArchT, when compared to the archaerhodopsin-3 (Arch), has more than three times light sensitive, thereby resulting in the more than a double of increase in tissue volume addressed by a typical single optical fiber[62]. Particularly, the ArchT action spectrum has a longer peak wavelength (580nm) than the Arch (550nm). This effect observed in ArchT is due to changes in the amino acid sequence in several places within the putative cytoplasmic and extracellular domains, however it does not alter the maximum current (~900 pA in vitro) and the kinetic of photocurrent rise and fall, which remains similar to Arch[62].

Somatostatin

Somatostatin (SOM, also known as STT) is a neuropeptide that is expressed in interneurons[65]. Regarding the output connectivity the SOM^+ interneurons target dendritic domains, allowing these neurons to efficiently control the inputs to their target cells[66]. The SOM^+ interneurons are characterized as adapting regular-spiking non-pyramidal cells (fire a train of action potentials subsequently to a pulse), or burst spiking non-pyramidal cells(fire action potentials only after the reach of a threshold)[67]. The SOM-IRES-Cre is active in many brain regions, including cortex, amygdala and brainstem[40].

To study these interneurons connectivity a SOM-Cre driver mouse line in combination with adeno-associated virus to deliver ChR2 can be used to mark these neurons light sensitive. The SOM-IRES-Cre mice express Cre recombinase in somatostatin-expressing neurons, without disrupting endogenous SOM expression, therefore Cre recombinase activity is observed in somatostatin positive neurons[74].

Several parameters for optogenetic manipulations have been reported when using the SOM^+ interneurons (**Supplementary Table I**).

Parvalbumin

Parvalbumin (PVa) is a calcium-binding protein that is expressed in GABAergic interneurons[67]. Contrary to the SOM^+ interneurons, the PVa^+ interneurons innervate target cells in the perisomatic domain.

The PVa^+ interneurons have multiple and long dendrites. Moreover, both the somata and the dendrites are densely covered with synapses. These properties allow these interneurons to receive multiple inputs from different afferent pathways, both from pyramidal cells and other interneurons[76]. In addition, the extensive arborization of the axons allows for a substantial divergent inhibitory output[76].

PVa^+ interneurons are normally fast-spiking, with a high-frequency train of action potential non-accommodating firing pattern, being reported to be involved both in feedforward and feedback inhibition[67,76]. The fast-spiking behaviour of the PVa^+ interneurons is mainly due to the high dendritic ratio of K^+ to Na^+ channels; in particular, the K^+ channels are mostly of the Kv3 type, which show a high activation threshold, fast activation and deactivation[76].

As previous, we will use a Cre driver mouse line in combination with adeno-associated virus to deliver chanelrhodopsin-2 (ChR2) to turn these neurons light sensitive. The PVa-IRES-Cre mice express Cre recombinase in parvalbumin-expressing neurons, without disrupting endogenous PVa^+ expression, therefore Cre recombinase activity is observed in PVa^+ neurons[74]. As for the SOM^+ interneurons several parameters for optogenetic manipulations have been reported when using the PVa^+ interneurons (**Supplementary Table II**).

Supplementary Table I – Summary of studies reviewed reporting optogenetic manipulation in cells expressing somatostatin

Mouse	Brain Area	Preparation	Pulse duration	Intensity	Frequency	Reference
Sst-IRES-Cre:: LSL-tdTomato	L2/3 Barrel cortex	*In vivo*, anesthetized animals	▪ 1 ms ▪ 1 ms (ISI 5 s) ▪ 1 ms	10-70 mW/mm^2 (mean ± SD: 32 ± 23 mW/mm^2)	▪ 1 Hz ▪ 50 Hz ▪ 20 Hz	Pala and Petersen, 2015[68]
SOM-Cre	Somatosensory Cortex L2/3 and L4	*Ex vivo*, Brain Slice	2 ms	0,2 - 1,0 mW		Xu *et* al., 2013[69]
SOM-Cre	Deep layer of the anterior cingulate cortex (ACC)	*In vivo*, Behaving animals	1 ms	100 mW/mm^2	10 Hz	Kvitsiani *et* al., 2013[70]
SOM-Cre	Basolateral Amygdala (BLA)	*In vivo*, Behaving animals	▪ 300 ms (2 s ISI) ▪ 1 s continuous	10 – 15 mW	0.5 Hz	Wolff *et* al., 2014[66]
SOM-Cre::GAD-EGFP	Basolateral Amygdala (BLA)	*Ex vivo*, Brain Slice	5 ms	10 mW		Wolff *et* al., 2014[66]
SOM-Cre::Thy1-EGFP	Motor Cortex	*In vivo*, Behaving animals	10 ms	40 mW	3 Hz	Chen *et* al., 2015[71]
SOM-Cre	Anterior Cingulate Cortex (ACC)	*In vivo*, Behaving animals	300 ms	20 - 25 mW/cm^2	0.5 Hz	Kang *et* al., 2015[72]
SOM-IRES-Cre	Primary visual cortex	*In vivo*, anesthetized animals	1 ms	4.1 mW /mm^2	40 Hz	Cottam *et* al., 2013[73]

Supplementary Table II – Summary of studies reviewed reporting optogenetic manipulation in cells expressing parvalbumin

Mouse	Brain Area	Preparation	Pulse duration	Intensity	Frequency	Reference
PV-IRES-Cre	Superior colliculus (SC)	Ex vivo, Brain Slice	10 ms	20 mW	10 Hz	Shang et al., 201577
PV-IRES-Cre	Superior colliculus (SC)	In vivo, Behaving animals	▪ 20 ms ▪ 20 ms ▪ 200 ms	20 mW 12 mW 20 mW	10 Hz 10 Hz 1 HZ	Shang et al., 201577
PV-ires-Cre	Dorsomedial prefrontal cortex	In vivo, Behaving animals	250 ms		0.9 Hz	Courtin et al., 201478
PV-ires-Cre	Basolateral Amygdala (BLA)	In vivo, Behaving animals	▪ 300 ms (2 s ISI) ▪ 1 s continuous	10 – 15 mW	0.9 Hz	Wolff et al., 201466
PV-Cre::GAD-EGFP	Basolateral Amygdala (BLA)	Ex vivo, Brain Slice	5 ms	10 mW	0.9 Hz	Wolff et al., 201466
PV-ires-Cre	CA3 area of the hippocampus	Ex vivo, Brain Slice	1-2 ms		▪ 20 Hz ▪ 50 Hz	Ledri et al., 201479
PV-Cre	Anterior Cingulate Cortex (ACC)	In vivo, Behaving animals	1-2 ms	2-6 mW	10 Hz	Kvitsiani et al., 201370
PV- Cre::Thy1-EGFP	Motor Cortex	In vivo, Behaving animals	10 ms	40 mW	3 Hz	Chen et al., 201571